Palaeogeography, Palaeoclimatology, Palaeoecology 280 (2009) 258–274

Contents lists available at ScienceDirect

Palaeogeography, Palaeoclimatology, Palaeoecology

journal homepage: www.elsevier.com/locate/palaeo

Late Weichselian and Holocene sedimentary environments and ice rafting in Isfjorden, Spitsbergen

Matthias Forwick *, Tore O. Vorren

University of Tromsø, Department of Geology, N-9037 Tromsø, Norway

ARTICLE INFO

Article history:
Received 6 October 2008
Received in revised form 16 June 2009
Accepted 16 June 2009
Available online 23 June 2009

Keywords:
Glacial sedimentary environments
Sea-ice rafting
Iceberg rafting
Fjord
Late Weichselian
Holocene

ABSTRACT

Multi-proxy analyses of two sediment cores from central Isfjorden were used to reconstruct the glacial history in central Spitsbergen during the Late Weichselian and the Holocene, and to relate iceberg rafting and sea-ice rafting to climatic and oceanographic changes in the north Atlantic region. A basal till was deposited beneath an ice stream prior to 12,700 cal. years BP (calendar years before the present). Several tidewater glaciers influenced the sedimentary environment during the Younger Dryas and probably already during the Allerød. The Younger Dryas cooling might be reflected by enhanced sea-ice formation and suspension settling, as well as reduced iceberg rafting. The final deglaciation was dominated by intense iceberg rafting. It terminated around 11,200 cal. years BP. Optimum Holocene climatic and oceanographic conditions with significantly reduced ice rafting occurred between c. 11,200 and 9000 cal. years BP. Ice rafting occurred almost exclusively from icebergs after 10,200 cal. years BP. The icebergs most probably originated from tidewater glaciers on east Spitsbergen, indicating the presence of a strong east–west temperature gradient at this time. An increase of iceberg rafting around 9000 cal. years BP, followed by enhanced sea-ice rafting, reflects the onset of a general cooling in the western Barents Sea–Svalbard region. Comparatively intense rafting from icebergs and sea ice between 9000 and 4000 cal. years BP is related to this cooling. A general reduction in ice rafting after 4000 cal. years BP is most probably the result of the enhanced formation of shore-fast and/or more permanent sea-ice cover, reducing the drift of icebergs and sea ice in the fjord. The results indicate that the palaeoenvironmental conditions on central Spitsbergen to a large degree depended on the oceanographic conditions in the western Barents Sea and west off Spitsbergen. However, climatic trends affecting Greenland and the entire north Atlantic region can also be identified.

1. Introduction and background

Climate modelling experiments indicate that the temperature increase during the next century will be particularly pronounced in the Arctic region (IPCC, 2007). However, the projections of future climate change are hampered because of the limited understanding of natural climate variability, so that it is important to study the climatic development of northern high latitudes during the Holocene (Renssen et al., 2005).

Numerous reconstructions of the Holocene palaeoclimatic and -oceanographic conditions from the north Atlantic region with sub-millennial time resolution are based on the analyses of ice cores, as well as terrestrial and 'open ocean' records (e.g. Werner, 1993; Svendsen and Mangerud, 1997; Johnsen et al., 2001; Sarnthein et al., 2001; Isaksson et al., 2003, 2005; Rohling and Pälike, 2005; Nesje et al., 2005; Ślubowska et al., 2005; Hald et al., 2007). However, reconstructions with similar time resolution from Spitsbergen fjords are sparse (Hald et al., 2004; Zajączkowski et al., 2004; Majewski and Zajączkowski, 2007; Hald and Korsun, 2008; Majewski et al., 2009).

Spitsbergen fjords are settings that are characterised by strong environmental gradients. On one hand, they are influenced by tidewater glaciers and partly covered by sea ice during winter. On the other hand, their oceanography is to a large degree affected by intrusions of the West Spitsbergen Current, one of the most distal parts of the North Atlantic Drift that transports relatively warm and saline Atlantic Water to the Arctic (Fig. 1; Svendsen et al., 2002; Saloranta and Haugan, 2004; Schauer et al., 2004; Cottier et al., 2007; Nilsen et al., 2008). Even minor changes in the intensity of the North Atlantic Drift will have a significant impact on the environmental conditions on Spitsbergen. For example can short-lasting increases in the inflow of Atlantic Water significantly reduce the formation of sea ice in the fjords during winter (Cottier et al., 2007). Due to their vicinity to sediment sources, Spitsbergen fjords provide unique settings for the study of variations in glacial activity and the influence of Atlantic Water and, hence, provide information about past environmental changes in the European Arctic with high temporal resolution.

The environmental conditions in large areas of the north Atlantic region improved rapidly after the Younger Dryas cooling as a result of

* Corresponding author. Tel.: +47 776 44453; fax: +47 776 45600.
E-mail address: Matthias.Forwick@uit.no (M. Forwick).

0031-0182/$ – see front matter © 2009 Elsevier B.V. All rights reserved.
doi:10.1016/j.palaeo.2009.06.026

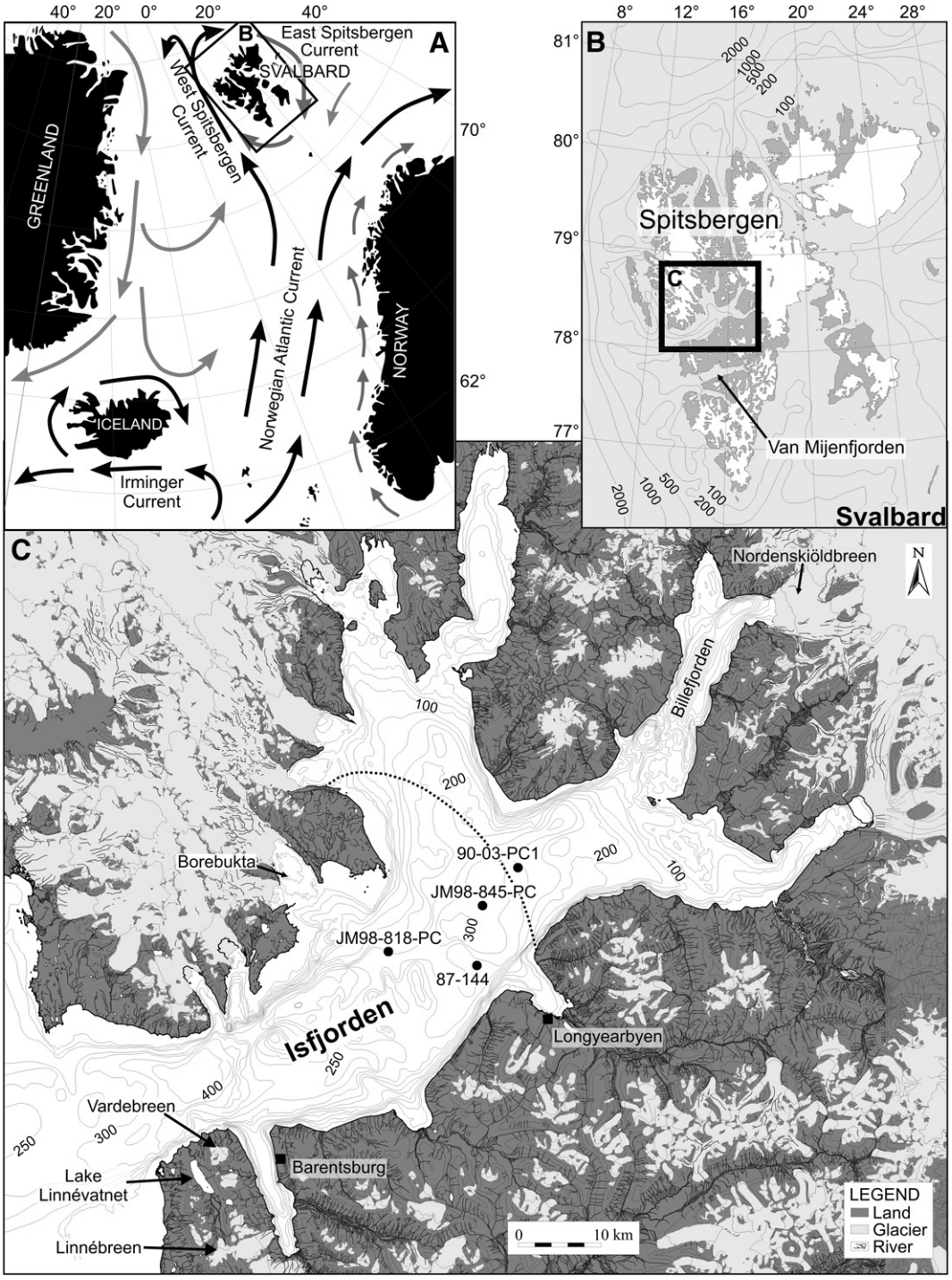

Fig. 1. A) Overview map of the north Atlantic region. Water currents mentioned in the text are indicated; B) Map of Svalbard; C) Bathymetry map of the Isfjorden area. Core locations (Table 1) and place names mentioned in the text are shown. The interval of the onshore contour lines is 500 m. The dotted line in central Isfjorden indicates the Younger Dryas minimum ice extent after Svendsen et al., 1996.

high solar insolation, increased meridional heat flux of Atlantic Water and ice-free conditions (e.g. Koç et al., 1993; Bauch et al., 2001; Duplessy et al., 2001; Klitgaard-Kristensen et al., 2001; Birks and Koç, 2002; Sarnthein et al., 2003; Ślubowska-Woldengen et al., 2007). The Holocene Climatic Optimum occurred during the first half of the Holocene. However, its estimated onset and duration varied with up to several thousand years, depending e.g. on latitude, the influence of the remnants of the Fennoscandian, Laurentide and Greenland ice sheets, as well as on the proxies applied (e.g. Koç et al., 1993; Duplessy et al., 2001; Johnsen et al., 2001; Klitgaard-Kristensen et al., 2001; Knudsen et al., 2004; Moros et al., 2004; Cortese et al., 2005; Nesje et al., 2005; Rasmussen, et al., 2007; Hald et al., 2007; Ślubowska-Woldengen et al., 2008). Shorter cooling intervals interrupted the warming trend during the early stages of the Holocene. These were most probably related to one or several factors including solar activity changes, increased explosive volcanism and internal feedback mechanisms in the Earth's climate system, as well as sudden fresh-water outbursts during the deglaciation of the Fennoscandian, Laurentide and

Greenland ice sheets (e.g. Hald and Hagen, 1998; Klitgaard-Kristensen et al., 2001; Nesje et al., 2004, 2005; Rohling and Pälike, 2005). Most, if not all, glaciers in southern Norway may have melted completely at least once between c. 8000 and 4000 cal. years BP (calendar years before the present; e.g. Nesje et al., 2005).

The subsequent, stepwise cooling is generally related to decreasing insolation, resulting in reduced heat flux from the Atlantic Water to high northern latitudes and, in consequence, decreasing sea-surface temperatures that led to increased sea-ice cover (e.g. Koç et al., 1993; Koç and Jansen, 1994; Klitgaard-Kristensen et al., 2001; Voronina et al, 2001; Birks and Koç, 2002; Nesje et al., 2005; Ślubowska-Woldengen et al., 2007). Simultaneously, increased influx of cool, low saline and δ^{18}O-depleted Arctic Waters to the eastern Barents Sea occurred (Hald et al., 1999; Duplessy et al., 2001; Lubinski et al., 2001). In Scandinavia, glaciers started to re-form/readvance between 6000 and 4000 cal. years BP (Nesje et al., 2005, 2008).

Spitsbergen fjords acted as pathways for fast-flowing ice streams draining the Late Weichselian Svalbard–Barents Sea Ice Sheet (e.g. Landvik et al., 1998, 2005; Ottesen et al., 2005). The mouth of Isfjorden (Fig. 1) was deglaciated at c. 14,100 cal. years BP and the final glacier retreat in the inner fjords terminated around 11,300 cal. years BP (e.g. Mangerud et al., 1992; Elverhøi et al., 1995; Svendsen et al., 1996; Mangerud et al., 1998; Lønne, 2005). The deglaciation pattern in Spitsbergen fjords and the behaviour of the glacier fronts during the Younger Dryas cooling is still poorly understood. Mangerud and Svendsen (1990), Svendsen and Mangerud (1992) and Mangerud and Landvik (2007) showed that local glaciers on western Spitsbergen were smaller during the Younger Dryas than during the Little Ice Age and that no evidence for a Younger Dryas readvance exists. It has been suggested that the tributaries of Isfjorden were occupied by outlet glaciers and that their fronts were located either in the inner main fjord (Mangerud et al., 1992) or "far out in the main fjord" (Svendsen et al., 1996, see Fig. 1C). Retarded glacio-isostatic uplift during the Younger Dryas (Forman et al., 1987; Landvik et al., 1987; Lehman and Forman, 1992) led Svendsen et al. (1996) to conclude that the glaciers in the inner parts of Isfjorden readvanced during this period. Boulton (1979) suggested a marked Younger Dryas glacier readvance in the Billefjorden area.

The chronology of the Holocene glacial activity in Spitsbergen fjords remains debatable. Whereas Svendsen and Mangerud (1997) did not find any glacial signal in Lake Linnévatnet and Billefjorden (for location see Fig. 1C) during the early and mid Holocene, Hald et al. (2004) inferred that central Spitsbergen was never completely deglaciated during the Holocene. Svendsen and Mangerud (1997) suggested that the glacier Linnébreen started to form approximately 4000–5000 years ago and that Nordenskiöldbreen in Billefjorden formed c. 3000–4000 years ago (for locations see Fig. 1C). However, Forwick and Vorren (2007) found indications that Vardebreen, c. 10 km north of Linnébreen (Fig. 1C), formed or increased in size already c. 7000 cal. years BP.

In this paper, we present data that provide new information about the environmental conditions in the largest fjord system on Spitsbergen during the past c. 13,000 years. We discuss temporal variations of iceberg rafting and sea-ice rafting and how these processes relate to climatic and oceanographic changes in the north Atlantic region.

2. Physiographic setting

The Isfjorden fjord system is the largest fjord system on the island Spitsbergen, Svalbard (Fig. 1). It is c. 100 km long, up to 425 m deep and it comprises the trunk fjord Isfjorden and thirteen tributary fjords and bays. The fjord system is surrounded by the second largest drainage basin on Spitsbergen (7309 km^2; Hagen et al., 1993). With a glacier coverage of about 40%, it is, however, the area with the least relative glacier cover on the island. Nine tidewater glaciers terminate into the fjord system.

The hydrography in Isfjorden is characterised by water masses of internal and external origin (Nilsen et al., 2008). Surface waters (mainly formed from glacial melt and river runoff during late spring and summer), local waters (increased salinity due to sea-ice formation) and winter-cooled waters originate in the fjords. Atlantic Water from the West Spitsbergen Current and Arctic-type water, a heavily modified extension of the East Spitsbergen Current, intrude into the fjord system through the mouth of Isfjorden (Fig. 1A; Nilsen et al., 2008).

Sea ice usually forms in the inner fjords on western Spitsbergen in December/January and starts to break up between April and July (Węsławski et al., 1995; Svendsen et al., 2002; Nilsen et al., 2008). However, the sea-ice conditions are strongly controlled by interactions with the atmosphere and ocean (Cottier et al., 2007).

The bedrock geology in most of the Isfjorden system is dominated by partly deformed sedimentary rocks of Devonian to Paleogene age (Dallmann et al., 2002). Intensely deformed metamorphic and sedimentary rocks of Proterozoic to Mesozoic age occur in the west. Smaller areas of volcanic and metamorphic rocks occur in the east and northeast. Unconsolidated Quaternary fluvial and marine sediments have been deposited in surrounding valleys and on raised strandflats (Dallmann et al., 2002).

3. Materials and methods

This study is based on the analysis of the two piston cores JM98-818-PC and JM98-845-PC (Fig. 1C; Table 1) that were retrieved with R/V "Jan Mayen" in 1998. The inner diameters of the cores are 10 cm. The plastic liner containing the interval between 168 cm and 267.5 cm in core JM98-818-PC was partly flattened due to the formation of vacuum during core sampling; the sediments of this section were partly disturbed. In core JM98-845-PC, the sediments were disturbed between approximately 20 cm and 25 cm, probably also as a consequence of vacuum generated during coring.

Prior to opening, the physical properties of the cores were measured in one-cm steps using a *GEOTEK Multi-Sensor Core Logger* (MSCL). The parameters included bulk density, magnetic susceptibility (loop sensor) and fractional porosity. After opening, the magnetic susceptibility was measured with a point sensor (Bartington MS2EI) in 0.5 cm intervals. Radiographs of half-core sections were acquired and described. Visual description was performed and colour information is based on the *Munsell Soil Color Chart*. The water content as well as the shear strength, using the fall-cone test (Hansbo, 1957), were estimated.

Grain-size analyses were performed on samples from core JM98-845-PC. Above 725 cm, the samples comprised 1 cm thick slices that were sampled every 10 cm, starting at 5 cm. Below 725 cm, samples had generally smaller and variable volumes, because of variable thicknesses of sampled strata. Sieves with mesh sizes of 63 μm, 125 μm, 250 μm, 500 μm, 1 mm, 2 mm, 4 mm and 8 mm were used. The fraction <63 μm was analysed with a *Micrometrics SediGraph 5100* in order to separate clay and silt. The boundary between clay and silt was set at 2 μm. Weight percentages of clay, silt and sand fractions of core JM98-845-PC are

Table 1
Overview of sediment cores that provide the basis for this study, and cores referred to in the text (see Fig. 1 for locations).

Core no.	Latitude [N]	Longitude [E]	Water depth [m]	Recovery [m]	Reference
JM98-818-PC	78°17.57′	14°48.17′	239	7.05	This study
JM98-845-PC	78°20.64′	15°18.11′	257	10.15	This study
87-144	78°16.6′	15°15.6′	228	?	Svendsen et al., 1992, 1996
90-03-PC1	78°22.77′	15°28.72′	216	?	Elverhøi et al., 1995; Svendsen et al., 1996

presented. We excluded grains larger than 2 mm from the calculations since the weight of one single large grain can bias the data.

Grains larger than 1 mm are regarded to be ice-rafted debris (IRD; compare with Hald et al., 2004), except in the basal till comprising unit I-T (see below). We counted their numbers in the grain-size distribution samples. The roundness of grains >1 mm was determined using a binocular. IRD fluxes were calculated for the uppermost 705 cm.

Fifteen AMS-radiocarbon dates of shells, snails and foraminifera were obtained. The targets were produced at the Radiological Dating Laboratory in Trondheim, Norway, and the measurements were carried out at the Ångström Laboratory in Uppsala, Sweden. A marine reservoir effect of 440 years was applied (Mangerud and Gulliksen, 1975). The radiocarbon ages were calibrated with the software programme *Calib Rev 5.0.1* (Stuiver and Reimer, 1993) using $\Delta R = 93 \pm 23$ (regional average for Spitsbergen; in marine reservoir correction database: http://radiocarbon.pa.qub.ac.uk/marine/). Results were obtained from the calibration data set *marine04.14C* of Hughen et al. (2004).

4. Results

Based on multi-proxy analyses of the two piston cores JM98-818-PC and JM98-845-PC (Fig. 1C; Table 1) we define five lithological units

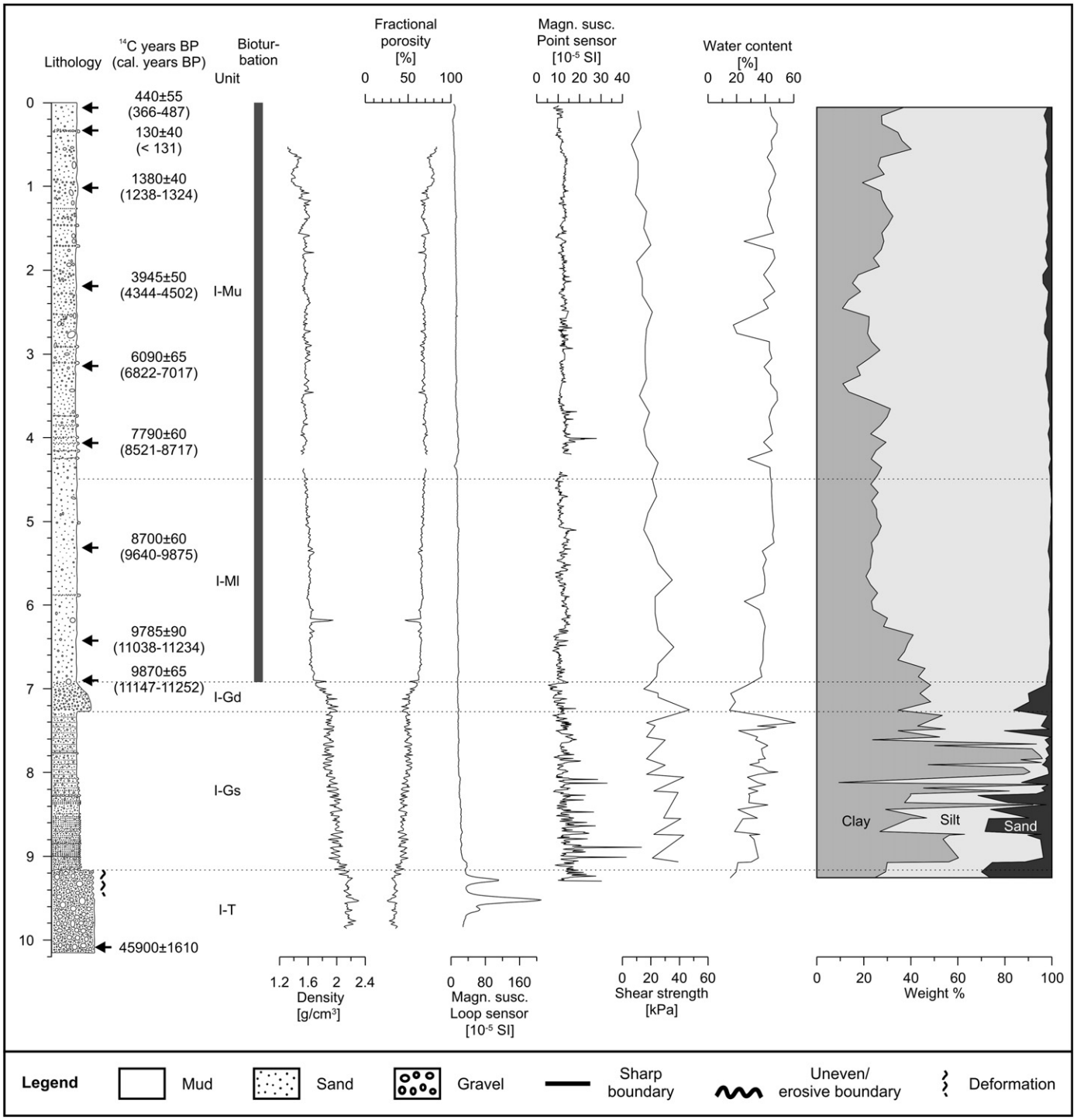

Fig. 2. Lithological log of core JM98-845-PC. Intervals of deformation, chronology, lithostratigraphic units, occurrence of bioturbation, as well as logs of the physical properties and grain-size distribution are presented. See Table 2 for more details about the physical properties.

for central Isfjorden (Figs. 2–4). A detailed overview about the lithological composition, sediment colour, as well as physical-properties and other parameters is given in Table 2.

4.1. Lithostratigraphy

4.1.1. Unit I-T — Basal till

Unit I-T occurs below 918 cm in core JM98-845-PC (Figs. 2, 3A; Table 2). It comprises a very dark greyish brown, massive diamicton with high clast content in a muddy matrix. Its upper boundary is sharp and uneven. Reliable shear-strength measurements with the fall-cone test could not be performed due to the high clast content. However, sticking a needle into the sediments revealed that the deposits are slightly overconsolidated in comparison to the other units. Both the bulk density and the magnetic susceptibility reach the highest values for the entire core (Fig. 2). The grains >1 mm in two grain-size distribution samples are predominantly angular (Fig. 6). Several deformed strata and patches of more reddish and brownish sediments occur above 948 cm. One shell fragment was dated to c. 46,000 ^{14}C BP (radiocarbon years before the present; Fig. 2; Table 3).

Because of the high clast content and overconsolidation we suggest that unit I-T is a basal till. Deformed strata may indicate that this unit was deposited beneath a fast flowing glacier/ice stream (Alley et al., 1986; Benn and Evans, 1996).

4.1.2. Unit I-Gs — Stratified glacimarine sediments

Unit I-Gs is present in both cores (Figs. 2, 3B, 4; Table 2). Its thickness is 190 cm in core JM98-845-PC and 393 cm in core JM98-818-PC, respectively. It is characterised by clast-bearing stratified mud with intercalated sandy strata. The colours vary between the three end members reddish brown, very dark greyish brown and very dark grey. Boundaries between strata are generally sharp or gradational. Some erosional boundaries occur in the lower parts of the unit, predominantly at the bases of the sandy strata. These sandy strata may be turbidites (see e.g. Mackiewicz et al., 1984; Powell, 1984; Powell and Molnia, 1989). The amount of sandy strata decreases upwards, coinciding with a general fining upward trend (Fig. 2). Some deformation occurs in core JM98-818-PC (Fig. 4; Table 2). This is supposed to be the result of mass-transport activity because of the core's location close to the slope off Borebukta (Fig. 1C).

The physical-property logs show generally cyclic fluctuations with slightly up-core decreasing bulk density and increasing fractional porosity (Figs. 2, 4). The fluctuations of the bulk-density logs and changes in the grey intensity on the X-radiographs (Fig. 3B) indicate that the stratification in unit I-Gs is partly related to variations in grain size. However, particularly in the upper parts of the unit, where the lithological changes are not as pronounced as in the lower parts, the sediment colour defines the stratification to a large degree. Because of the stratification and the high clast content, we suggest that unit I-Gs was deposited in a glacimarine environment where sediment input occurred from multiple sources.

4.1.3. Unit I-Gd — Clast-rich glacimarine diamicton

Unit I-Gd comprises a 30–35 cm thick upward fining, massive and clast-rich diamicton with a muddy matrix (Figs. 2, 3C, 4; Table 2). It has gradational upper and lower boundaries. The values of the physical properties, except of the fractional porosity and the water content, decrease up-core. Close to the top of the unit, the lowest magnetic-susceptibility values for the entire core were measured. Within the lowermost 20–25 cm, the sediment colour is a mixture of

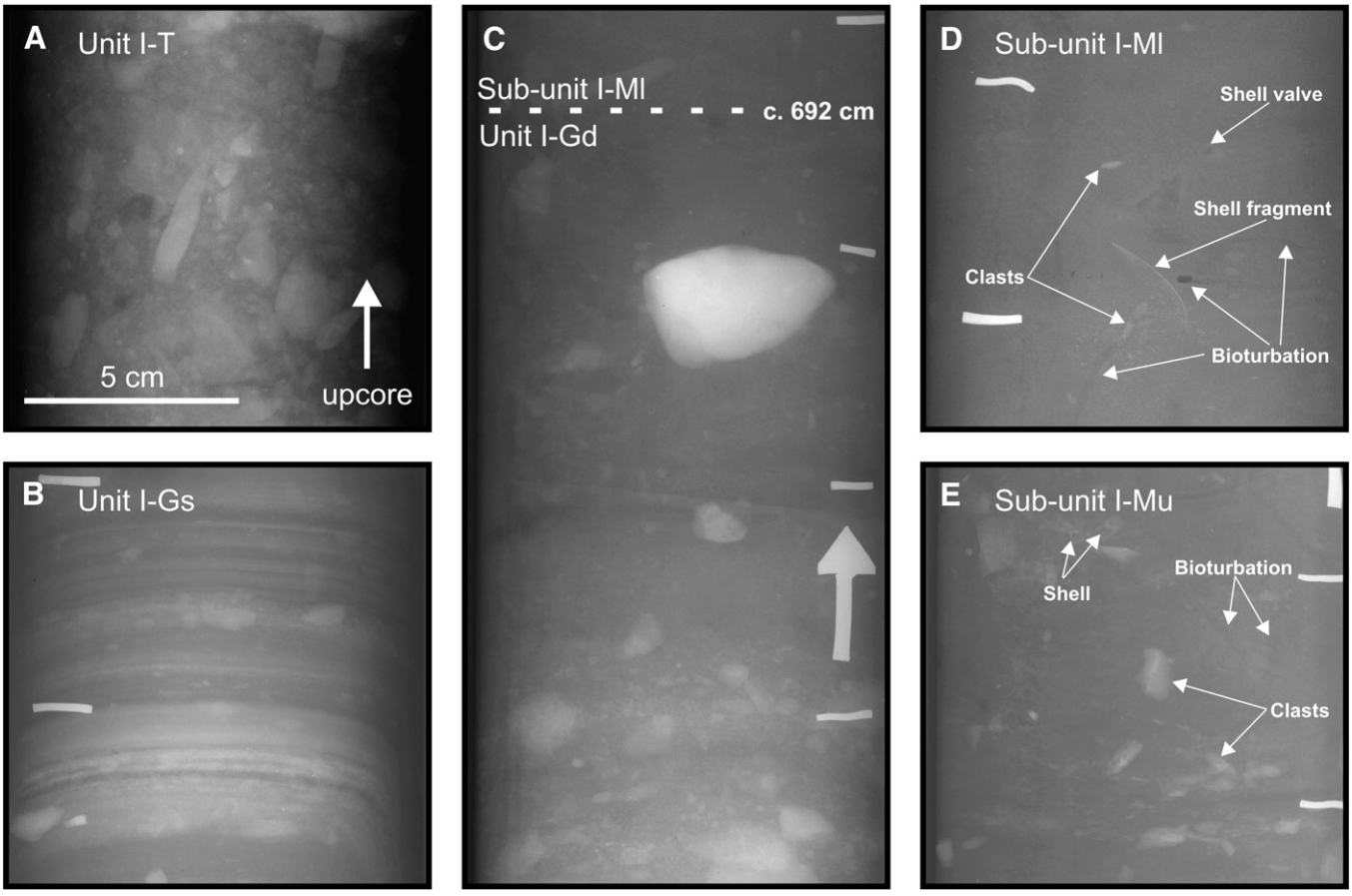

Fig. 3. Radiographs from core JM98-845-PC (lighter grey tones reflect higher density); A) Basal till (I-T); B) Stratified glacimarine sediments (I-Gs); C) Glacimarine diamicton (I-Gd); D) Massive mud (lower glacial activity; I-MI); E) Massive mud (higher glacial activity; I-Mu).

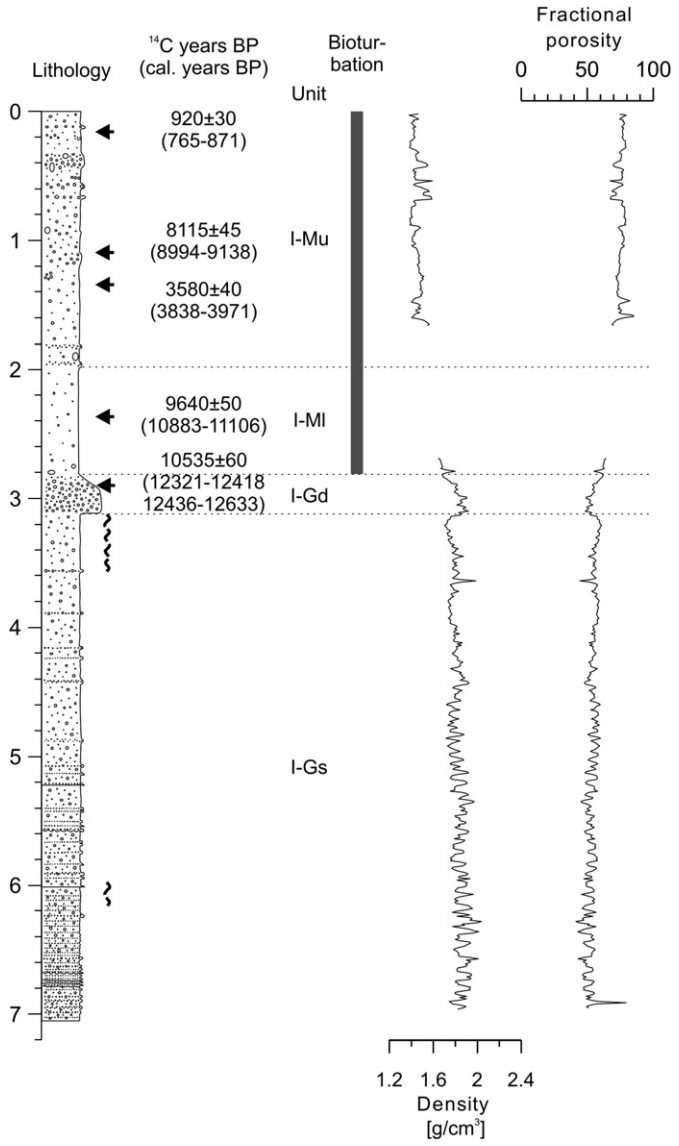

Fig. 4. Lithological log of core JM98-818-PC. Intervals of deformation, chronology, lithostratigraphic units, occurrence of bioturbation, as well as bulk density and fractional porosity are shown. The legend is shown on Fig. 2. See Table 2 for more details about the physical properties.

the reddish–greyish–brownish colours of unit I-Gs. However, more distinct strata of the single colours occur occasionally. The sediment colour changes gradually to very dark grey about 10 cm below the top of the unit. One radiocarbon date of benthic foraminifera from the upper parts of the unit in core JM98-818-PC provided an age of 10,535 ± 60 ^{14}C BP (Fig. 4; Table 3).

We suggest that unit I-Gd comprises a glacimarine diamicton that was deposited close to the end of the last glacial, rather than a basal till (unit I-T), because 1) the gradational boundaries indicate that this diamicton is part of a continuous sedimentation record linking the Late Weichselian stratified glacimarine sediments (unit I-Gs) with the Holocene mud (Unit I-M; for chronology see Section 4.2, below; Figs. 2, 3); 2) the undrained shear strength is similar to the shear strengths in the surrounding units, indicating that it is not over-consolidated (Fig. 2).

4.1.4. Unit I-M — massive glacimarine sediments

Unit I-M is the uppermost unit in both cores. It comprises bioturbated massive mud with clasts (Figs. 2, 3D, E, 4; Table 2). The amount of clasts is significantly less than in unit I-Gd. Black mottles occur on fresh surfaces. They disappear and the sediment colour changes to very dark grey when the sediment surface is exposed to air. Paired shells, shell fragments, snails and foraminifera are present. The unit is divided into the sub-units I-Ml (lower) and I-Mu (upper), respectively. Sub-unit I-Ml is characterised by lower clast contents but larger amounts of organic material, compared to sub-unit I-Mu (Figs. 2, 3D, E, 4). We suggest that unit I-M has been deposited in a glacimarine environment where sub-unit I-Ml reflects lower and sub-unit I-Mu higher glacial activity, respectively. Four radiocarbon dates from sub-unit I-Ml provided ages between 9870 ± 65 and 8700 ± 60 ^{14}C BP and nine radiocarbon dates from sub-unit I-Mu gave ages of maximum 8115 ± 45 ^{14}C BP (Figs. 2, 4; Table 3).

4.2. Chronology

The shell fragment from the basal till (unit I-T) was dated to c. 46,000 ^{14}C BP (Fig. 2; Table 3). This indicates that it lived during the Kapp Ekholm interstadial (Mangerud et al., 1998) or older interstadials, and that it was reworked during younger glacial periods. We suggest that the basal till was deposited during the last glacial, because 1) it is the only till in our record, and 2) older deposits were most probably removed by glaciers occupying the fjord (e.g. Hooke and Elverhøi, 1996).

Two radiocarbon dates from the deposits that are correlated with the overlying stratified glacimarine deposits (unit I-Gs; for correlation see Section 4.3, below) imply that the till was deposited prior to 10,585 ± 90 ^{14}C BP (c. 12,700 cal. years BP; Table 3; Elverhøi et al., 1995; Svendsen et al., 1996).

Very few foraminifera tests were found in the glacimarine deposits of unit I-Gs, so that no radiocarbon date could be obtained from our material. We suggest, however, that its deposition commenced after the deglaciation of the mouth of Isfjorden at 12,300 ^{14}C BP (c. 14,100 cal. years BP; Mangerud et al., 1992). Based on the correlation with the laminated glacimarine mud described by Elverhøi et al. (1995) and Svendsen et al. (1996; see Section 4.3, below), we infer that its deposition commenced before 10,585 ± 90 ^{14}C BP (c. 12,700 cal. years BP; Table 3). This indicates that the sediments were deposited during the Younger Dryas and probably also during the Allerød.

One radiocarbon date from the upper parts of unit I-Gd of 10,535 ± 60 ^{14}C BP (Fig. 4; Table 3) suggests that most of the clast-rich glacimarine diamicton was deposited during the early stages of the Younger Dryas. It should be noted that our date and the date of 10,395 ± 140 ^{14}C BP (Table 3; Svendsen et al., 1992, 1996) from deposits correlated with the underlying unit I-Gs show an age inversion. However, we assume that both dates are reliable, because the calibrated ages reveal that the dating material could have been deposited in the correct chronological order.

Whereas the four dates from sub-unit I-Ml have early Holocene ages, are the dates from sub-unit I-Mu of mid and late Holocene age (Figs. 2, 4; Table 3). When assuming a linear sedimentation rate between 8700 ± 60 and 7790 ± 60 ^{14}C BP in core JM98-845-PC (Fig. 2; Table 3), the transition from unit I-Ml to I-Mu occurred around 8100 ^{14}C BP (c. 9000 cal. years BP).

The material sampled from 109 to 110 cm in core JM98-818-PC provided an age that is significantly older than the age from 135 to 136 cm (Fig. 4; Table 3). We suppose that the material from 109 to 110 cm has been reworked and therefore disregard the result. The dates from sub-unit I-Mu in core JM98-845-PC show generally decreasing ages up-core and are assumed to provide reliable ages (Fig. 2; Table 3). However, we disregard the uppermost two dates, because 1) the date from 33 cm (130 ^{14}C BP) provides an invalid age for the calibration (Hughen et al., 2004); 2) the material from 6 cm (440 ^{14}C BP) was sampled in the vicinity of the disturbed section between c. 20 cm and 25 cm, and because it was sampled close to the core top that most probably has been disturbed during coring.

Table 2
Overview of characteristics and physical properties of the lithological units in the cores JM98-818-PC and JM98-845-PC, as well as their ages and genesis.

Parameter	Lithological unit				
	I-T	I-Gs	I-Gd	I-Ml	I-Mu
Core JM98-845-PC (10.15 m)	918 cm—end of core	728 cm–918 cm	692 cm–728 cm	c. 450 cm–692 cm	Top of core–c. 450 cm
Core JM98-818-PC (7.05 m)	Absent	312 cm—end of core	282 cm–312 cm	c. 198 cm–282 cm	Top of core–198 cm
Lithology	Massive, clast-rich diamicton with muddy matrix	Clast bearing stratified mud with intercalated sandy strata 1 mm to 6 cm thick strata with sharp or gradational boundaries Some erosional boundaries in lower part of unit, mainly at bases of sandy strata	Upward fining massive, clast rich diamicton with muddy matrix	Massive mud with clasts	Massive mud with clasts
Clast amount, size and shape	High amounts <5 cm Angular to rounded	Scattered and in layers Gen. <3 cm, but one 5 cm Angular to rounded	High amounts Up to 3 cm Angular to rounded	Scattered Generally<1 cm, but single clasts up to c. 5 cm Angular to rounded	Generally scattered, some intervals with higher amounts Generally<3 cm, but single clasts up to c. 5 cm Angular to well rounded
Colour (colour codes from *Munsell Soil Color Chart*)	Very dark greyish brown (10YR 3/2)	Reddish brown (5YR 3/2) Dark grayish brown (10YR 3/2) Very dark grey (10YR 3/1)	Lowermost 20–25 cm: Mixture of reddish–greyish–brownish colours of unit I-Gs; more distinct strata of single colours can occur Uppermost c. 10 cm: gradual (up-core) change to very dark grey (2.5 3/1)	Black mottles on fresh surfaces Change to very dark grey (2.5Y 3/1) when exposed to air	Black mottles on fresh surfaces Change to very dark grey (2.5Y 3/1) when exposed to air
Bulk density [g/cm^3]	2.0–2.3	1.7–2.1	1.7–2.0	1.5–2.0	1.3–1.7
Fractional porosity [%]	26–42	31–61	42–62	46–70	62–83
Magn. susc. (loop) [10^{-5} SI]	28–210	12–37	13–18	14–19	7–18
Magn. susc. (point sensor) [10^{-5} SI]	Not possible to measure	8-49/5-51 (core 845/core 818)	5-18/9-33	7-18/8-37	8-28/5-58
Shear strength [kPa]	Not possible to measure Stiff appearance when sticking a needle into the sediment	17–53	15–47	15–36	6–25
Water content [wt.%]	< 20	19–61	15–28	25–46	18–49
Lower unit boundary	Not recovered	Sharp and uneven	Gradational	Gradational	Gradational
Upper unit boundary	Sharp and uneven	Gradational	Gradational	Gradational	Top of cores
Deformation	Several deformed strata of more reddish and brownish sediments above 948 cm	Some folding and faulting in core JM98-818-PC (c. 357–312 cm; 615–597 cm)	Some folding in core JM98-818-PC	Not observed	Not observed
Bioturbation	Absent	Absent	Absent	Highest intensity in core	Second highest intensity in core
Datable material	One shell fragment	Very few foraminifera tests	Some foraminifera	Highest amount in core (e.g. paired shells, snails, foraminifera)	Second highest amount in core (e.g. paired shells, snails, foraminifera)
Age and genesis	Late Weichselian basal till	Late Weichselian glacier-proximal glacimarine sediments	Late Weichselian glacier-distal glacimarine diamicton	Early Holocene distal glacimarine mud–lower glacial activity	Mid/Late Holocene distal glacimarine mud–higher glacial activity

Table 3
Radiocarbon ages and calibrated ages obtained from the cores JM98-845-PC and JM98-818-PC as well as selected published ages.

Core	Depth [cm]	Material	Lab. No.	^{14}C age (± 2σ)	Calibrated age BP (1σ)	Calibrated age BP (2σ)	Lith. unit	Reference
JM98-845-PC	6	*Astarte sulcata* (paired)	TUa-4798	440 ± 55	366–487	298–508	I-Mu	This study
JM98-845-PC	33	*Yoldiella lucida* (paired)	TUa-4799	130 ± 40	Invalid	Invalid	I-Mu	This study
JM98-845-PC	102	*Bathyarca glacialis* (paired)	TUa-4800	1380 ± 40	1238–1324	1177–1368	I-Mu	This study
JM98-845-PC	219–220	*Yoldiella lenticula* (paired)	TUa-4801	3945 ± 50	4344–4502	4238–4564	I-Mu	This study
JM98-845-PC	314	*Yoldiella (lenticula)* (presumably paired)	TUa-4802	6090 ± 65	6822–7017	6752–7130	I-Mu	This study
JM98-845-PC	406–407	*Yoldia hyperborea* (paired)	TUa-4803	7790 ± 60	8521–8717	8436–8854	I-Mu	This study
JM98-845-PC	530–531	*Yoldiella lenticula* (paired)	TUa-4804	8700 ± 60	9640–9875	9536–9967 9972–10001	I-Ml	This study
JM98-845-PC	642–643	*Nuculana minuta* (paired)	TUa-4805	9785 ± 90	11038–11234	10785–11307	I-Ml	This study
JM98-845-PC	690	*Opistobranchia* indet. (fragments)	TUa-4806	9870 ± 65	11147–11252	11097–11360	I-Ml	This study
JM98-845-PC	1008–1009	*Astarte* sp.? (fragments)	TUa-4807	45900 + 1800/−1700	–	–	I-T	This study
JM98-818-PC	17	*Turitella communis* (whole)	TUa-5195	920 ± 30	765–871	720–904	I-Mu	This study
JM98-818-PC	109–110	*Yoldiella lenticula* (paired)	TUa-5194	8115 ± 45	8994–9138	8969–9244	I-Mu	This study
JM98-818-PC	135–136	*Yoldiella lenticula* (paired)	TUa-5193	3580 ± 40	3838–3971	3778–4066	I-Mu	This study
JM98-818-PC	235.5–238	*Yoldia hyperborea* (fragments)	TUa-5192	9640 ± 50	10883–11106	10735–11132	I-Ml	This study
JM98-818-PC	289–291	Foraminifera, several species, predominantly *Nonion labradoricum*	TUa-5191	10535 ± 60	12321–12418 12436–12633	12117–12140 12177–12689	I-Gd	This study
87-144	362	Shell indet.	Ua-757	10395 ± 140	11910–12389 12475–12580	11425–11490 11617–12710	I-Gs	Svendsen et al., 1992, 1996
90-03-PC1	255–265	Foraminifera, several species	TUa-442	10585 ± 90	12352–12689	12121–12134 12182–12793	I-Gs	Elverhøi et al., 1995; Svendsen et al., 1996

Even though we obtained radiocarbon dates from both cores (Figs. 2, 4; Table 3), our chronology for the environmental reconstructions during the Holocene are exclusively based on the dates from core JM98-845-PC because 1) the Holocene section in this core is more than twice as thick as in core JM98-818-PC (Figs. 2, 4; Table 2), and therefore provides higher temporal resolution; 2) parts of the Holocene section in core JM98-818-PC were disturbed during sampling (see Section 3); 3) we found signs of reworking of the sediments in core JM98-818-PC (deformed strata in unit I-Gs, age reversal in unit I-Mu; Fig. 3; Table 2).

4.3. Lithostratigraphic correlation

Elverhøi et al. (1983, 1995) and Svendsen et al. (1992, 1996) published lithological data from central Isfjorden. They distinguish three lithological units. Elverhøi et al. (1983) suggested that "ice-front deposits" are covered with "interbedded proximal deposits" (Fig. 5A). The latter are overlain by "homogenous distal mud/basin mud". Svendsen et al. (1992, 1996) and Elverhøi et al. (1995) suggested that a till is overlain by laminated (glacimarine) mud and olive grey mud (Fig. 5B). The till was deposited before 15 to 10 ^{14}C ka BP (thousands of

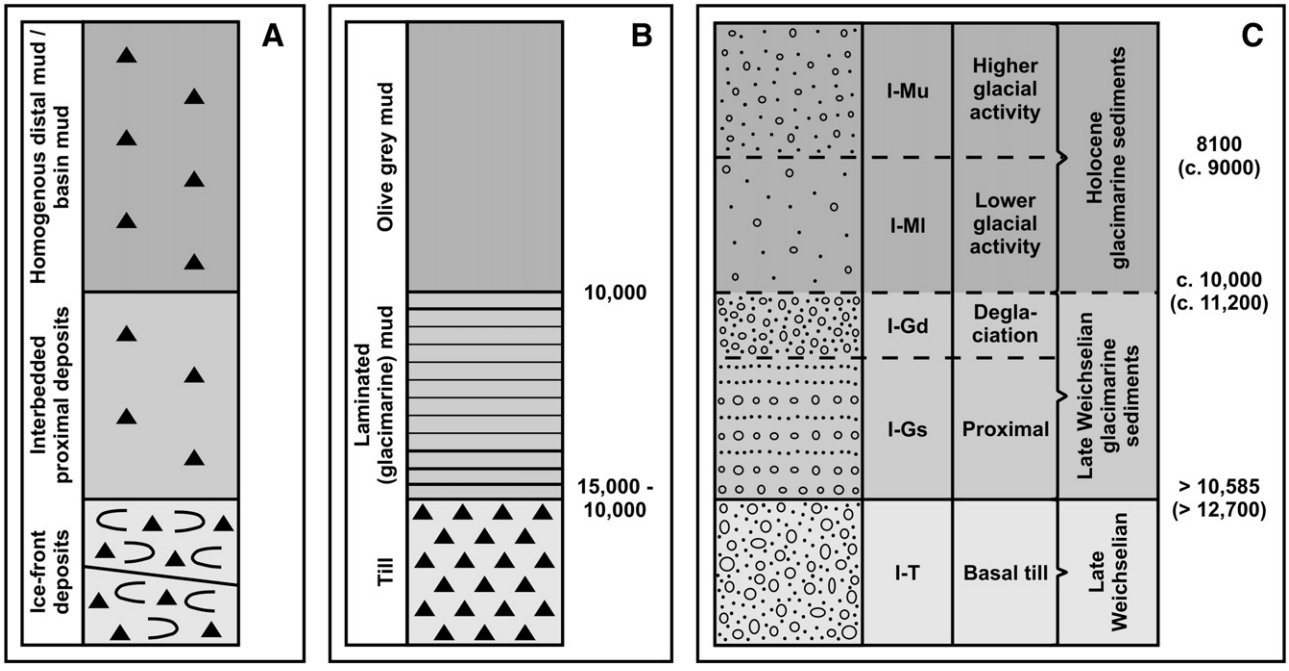

Fig. 5. A) Lithostratigraphy is Isfjorden modified after Elverhøi et al. (1983); B) Lithostratigraphy modified after Svendsen et al. (1992, 1996) and Elverhøi et al. (1995). The chronology to the right shows radiocarbon years before the present; C) Lithostratigraphy for central Isfjorden based on this study. The lithology (left column), lithological units, sedimentary environments, as well as a chronology (right column and numbers to the right) are indicated. Dots in the lithology column indicate the occurrence of sand, circles symbolise gravel. Dashed horizontal lines reflect gradational boundaries. The solid horizontal line indicates the sharp boundary between the basal till and the proximal glacimarine deposits. The numbers to the right are radiocarbon years before the present and calendar years before the present (in brackets).

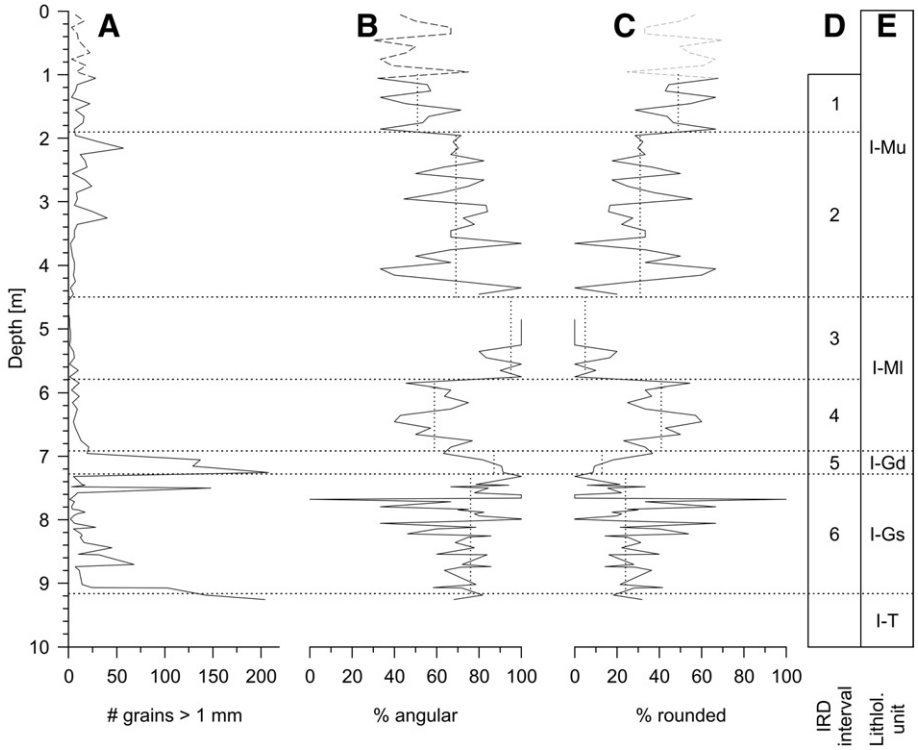

Fig. 6. A) Number of grains >1 mm in grain-size distribution samples from core JM98-845-PC; B) Percentages of angular grains; C) Percentages of rounded grains; D) IRD intervals; E) lithological units. Dotted vertical lines in B and C mark the average percentages in the IRD intervals (see also Table 4). Values for the uppermost c. 1 m are shown with dashed lines, because this interval is most probably disturbed (see Section 4.4).

radiocarbon years before the present), the laminated mud was deposited prior to 10 ^{14}C ka BP and the olive grey mud after 10 ^{14}C ka BP. Radiocarbon ages of 10,585 ± 90 ^{14}C BP and 10,395 ± 140 ^{14}C BP were obtained from the stratified glacimarine sediments (Table 3; Svendsen et al., 1992; Elverhøi et al., 1995; Svendsen et al., 1996).

The following lithological units from our study, and the records of Elverhøi et al. (1983, 1995) and Svendsen et al. (1992, 1996) can be correlated based on their lithologies, stratigraphic positions and chronologies (Fig. 5): I-T and the ice-front deposits/till; I-Gs and the interbedded proximal deposits/laminated (glacimarine) sediments; I-M and the homogenous distal mud/olive grey muds.

Our data allow the following improvements to the existing lithostratigraphy (Fig. 5C): 1) A massive glacimarine diamicton (unit I-Gd) separates units I-Gs and I-M; 2) we are able to sub-divide the glacimarine muds into lower (I-Ml) and upper (I-Mu) muds.

4.4. Sedimentation rate

The highest sedimentation rate in central Isfjorden during the Holocene occurred prior to c. 8800 cal. years BP (Fig. 8B, below). At that time, it dropped by approximately 50%. Another less pronounced decrease to the lowest Holocene values occurred around 7000 cal. years BP. The rate remained low until c. 1300 cal. years BP when it doubled.

A marked drop in the sedimentation rate in van Mijenfjorden (for location see Fig. 1B) occurred also around 8800 cal. years BP (Hald et al., 2004). However, an increase in the sedimentation rate that is comparable to the increase in Isfjorden around 1300 cal. years BP could not be detected in van Mijenfjorden. Because the increase appears unrealistically high and because parts of the uppermost sediment column of core JM98-845-PC are disturbed (see Section 3), we disregard the chronology for the last 1300 years (uppermost c. one meter) for further discussions.

4.5. Ice-rafted debris (IRD)

4.5.1. Amount and shape

Ice-rafted debris (grains>1 mm) was counted in the grain-size distribution samples from core JM98-845-PC (Figs. 6, 7). The number of grains per sample varies between 0 and 208; the average number of grains per sample is approximately 20 (note that the sample volumes are variable below 725 cm; see Section 3). No clasts were found in the samples 455–456 cm, 465–466 cm and 475–476 cm, respectively. However, the radiographs reveal scattered clasts around the sampled depths.

We divided the grains into two groups: one group comprising "angular" grains (including angular and sub-angular grains), and the other group containing "rounded" grains (including sub-rounded, rounded and well-rounded grains; Figs. 6–8; Table 4). The percentages

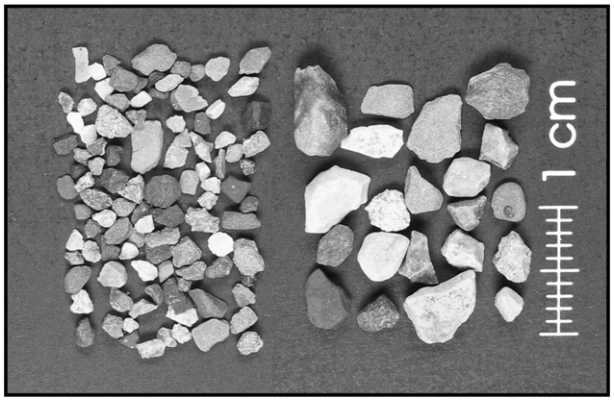

Fig. 7. Examples of ice-rafted debris 715–716 cm in core JM98-845-PC (left: 1–2 mm fraction; right: 2–4 mm fraction).

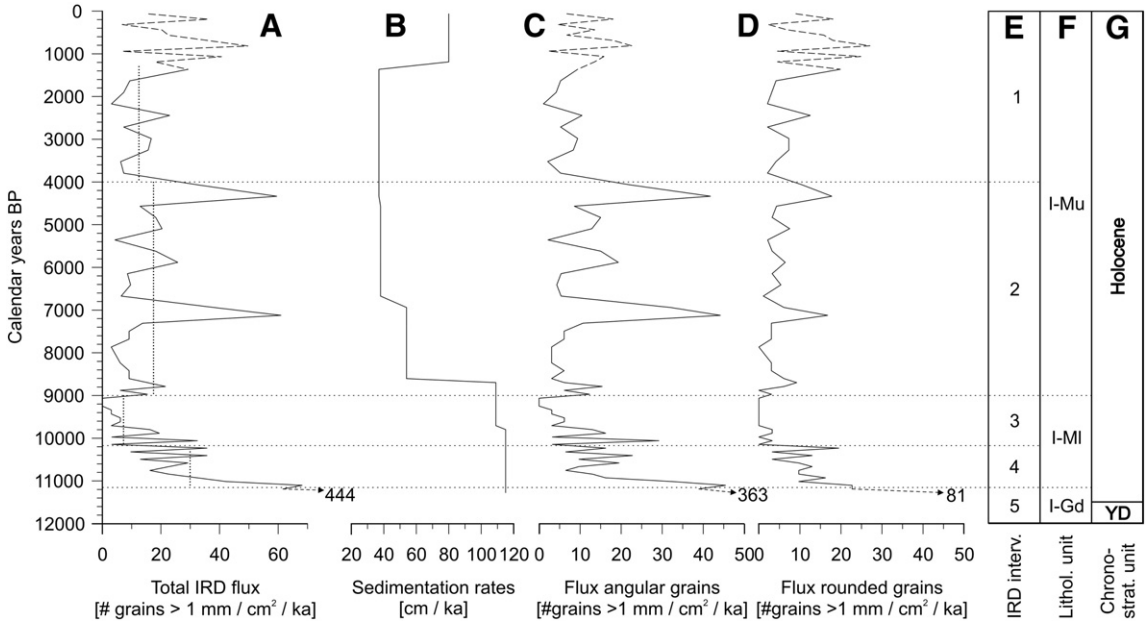

Fig. 8. A) IRD flux in central Isfjorden (dotted vertical lines indicate average fluxes; see also Table 4); B) Sedimentation rates during the past c. 11,300 calendar years; C) Percentages of more angular grains; D) Percentages of more rounded grains; E) IRD intervals; F) Lithological units; G) Chronostratigraphic units (YD=Younger Dryas). The dashed lines in the upper parts A, C and D indicate apparent IRD fluxes for the last c. 1300 years. They are not further discussed in the text, because of probable disturbance of the sediments (see Section 4.4).

of the two groups fluctuate, but angular grains generally dominate. Based on the average percentages of angular and rounded grains we distinguish six intervals of ice rafting. The intervals IRD-1 and IRD-2 occur in the lithological sub-unit I-Mu, IRD-3 and IRD-4 in sub-unit I-Ml, IRD-5 in unit I-Gd and IRD-6 in unit I-Gs, respectively (Figs. 6, 8; Table 4).

An overall upward decrease in the percentage of rounded grains occurs in interval IRD-6 (Fig. 6). However, more pronounced fluctuations and comparatively high percentages occur between c. 768 and 822 cm. Interval IRD-5 is characterised by increasing percentages of rounded grains (Figs. 6, 8; Table 4). Interval IRD-4 comprises moderately high and fluctuating percentages of rounded and angular clasts. A marked change in the clast roundness occurs at the boundary between the intervals IRD-4 and IRD-3. Interval IRD-3 is characterised by the highest percentage of angular clasts in the entire core. Marked fluctuations occur in interval IRD-2, in particular in the lower part. Whereas angular grains dominate in interval IRD-2 is the average ratio of angular to rounded grains in interval IRD-1 almost equal (Figs. 6, 8; Table 4).

4.5.2. IRD flux

The IRD fluxes for the top of the glacimarine diamicton (unit I-Gd) and the Holocene muds (units I-Ml and I-Mu) were calculated, based on the sedimentation rates in core JM98-845-PC (Fig. 8; Table 4). The fluxes at the top of unit I-Gd were estimated from an assumed continuous sedimentation rate below 690 cm.

Between c. 11,300 and c. 9300 cal. years BP, the IRD fluxes decreased from the highest values of 444 grains>1 mm/cm^2/ka (ka = thousands of calendar years) to zero (Fig. 8A). The most significant drop occurred between 11,300 and c. 10,800 cal. years BP. It was followed by decreasing and frequently fluctuating fluxes until 9700 cal. years BP. The flux decreased further between 9700 and 9300 cal. years BP. Based on the calculations it seems that no ice-rafting occurred between c. 9300 and 9000 cal. years BP. However, scattered clasts on the X-radiographs indicate that some ice rafting took place during this period. An increase in IRD flux occurred from c. 9000 to 8800 cal. years BP. The time between c. 9000 and 4000 cal. years BP is characterised by relatively high and oscillating IRD fluxes. The average IRD flux during this time was 17.5 grains>1 mm/cm^2/ka (Table 4). Fluxes of 12.5 grains>1 mm/cm^2/ka occurred between c. 4000 and c. 1300 cal. years BP. We did not include IRD fluxes for the past 1300 years (uppermost c. 1 m of the core) into this study, because of the unrealistically high sedimentation rate (Fig. 8B; see Section 4.4).

The fluxes of angular and rounded grains generally fluctuated synchronously (Fig. 8). However, three intervals of asynchronous fluctuations should be noted: 1) around 10,200 cal. years BP, when the flux of rounded grains dropped to almost zero, while the flux of angular grains continued to fluctuate; 2) An increase in angular grains between 9000 and 8800 cal. years BP was substituted by an increase in rounded grains between 8800 and 8600 cal. years BP; 3) a peak in the IRD flux around 5800 cal. years BP was almost exclusively related to the increase in the flux of angular grains.

Table 4
Characteristics of IRD intervals. Fluxes are shown in [# grains>1 mm/cm^2/ka].

IRD interval	Depth [m] in core JM98-845-PC	Age [cal. BP] or chronozone	% angular grains	% rounded grains	Average IRD flux	Average flux angular grains	Average flux rounded grains	Litho-unit
1	~1.00–1.90	1300–4000	51	49	12.53	6.05	6.47	I-Mu
2	1.90 to ~4.50	4000–9000	69	31	17.51	12.36	5.15	I-Mu
3	~4.50–5.80	9000–10,200	95	5	7.40	6.65	0.74	I-Ml
4	5.80–6.92	10,200–11,200	59	41	29.79	17.99	11.80	I-Ml
5	6.92–7.27	Late Younger Dryas/ early Preboreal	87	13	–	–	–	I-Gd
6	7.27–9.17	Younger Dryas and probably older	76	24	–	–	–	I-Gs

5. Discussion

5.1. Iceberg-rafted vs. sea-ice rafted debris

Ice rafting can occur by icebergs and sea ice. The size of the rafted material can occasionally be used to infer the type of transportation in shore-distal settings, i.e. larger particles are more likely to be deposited from icebergs (e.g. Gilbert, 1990; Knies et al., 2001). However, since core JM98-845-PC was retrieved from the central parts of Isfjorden, the setting is rather proximal, and we do not regard the grain size as a proxy for the distinction between iceberg-rafted and sea-ice rafted debris in our study.

Another parameter that might be used is the grain shape. Iceberg-rafted debris is angular to rounded, and sea-ice rafted debris is usually more rounded (Gilbert, 1990; Goldschmidt et al., 1992; Lisitzin, 2002). However, sea-ice rafted debris in polar settings can also be of a more angular type (Gilbert, 1990 and references therein). Hence, an unequivocal distinction between iceberg-rafted debris and sea-ice rafted debris remains problematic (Gilbert, 1990; Dowdeswell et al., 1998).

Based on the results of our study, we infer that iceberg-transported material in central Isfjorden has generally higher percentages of angular grains than sea-ice transported material, because: 1) Unit I-Gd/interval IRD-5 comprises a glacimarine diamicton that reflects the major and rapid retreat of the glacier fronts from central Isfjorden at the end of the Late Weichselian glaciation. The retreat occurred mainly through iceberg calving (see Section 5.3, below). The unit/interval is characterised by high IRD flux and comparatively high percentages of angular grains (on average 87%; Figs. 6, 8; Table 4); 2) In Section 5.4 (below), we infer that the period between c. 10,200 and 8800 cal. years BP is characterised by warm surface waters, suppressing the formation of sea ice. Accordingly, the IRD was mainly iceberg derived. The grains >1 mm that were deposited during this period are almost exclusively angular (Figs. 6, 8; Table 4); 3) The samples from the basal till (unit I-T) indicate that glacier-derived material is mainly angular (Fig. 6).

5.2. Late Weichselian glaciation

We suggest that the basal till (unit I-T) at the base of core JM98-845-PC (Figs. 2, 3; Table 2) was deposited beneath an ice stream that drained the Late Weichselian Svalbard-Barents Sea Ice Sheet through Isfjorden during the last glacial (compare with Ottesen et al., 2005). High magnetic susceptibility indicates that at least some material derived from areas other than in the overlying units. Even though restricted areas of volcanic and metamorphic rocks occur in areas that presently supply sediments to central Isfjorden (Dallmann et al., 2002), the magnetic susceptibility of the units overlying the till remains below 40 10^{-5} SI (loop sensor) and 60 10^{-5} SI (point sensor), respectively. Hence, the material with the high magnetic susceptibility may have its origin north of Billefjorden where e.g. granitic rocks and mica gneisses occur (Dallmann et al., 2002), or further away. This suggests a transport distance of at least c. 50 km.

5.3. Late Weichselian/earliest Holocene deglaciation

The stratified glacimarine sediments (unit I-Gs; Figs. 2, 3) covering the basal till, as well as the clast-rich glacimarine diamicton (unit I-Gd) were deposited during a period when the glacier fronts retreated from the mouth of Isfjorden and to the heads of its tributaries (e.g. Mangerud et al., 1992; Elverhøi et al., 1995; Svendsen et al., 1996; Mangerud et al., 1998; Lønne, 2005).

We suggest that unit I-Gs was deposited in a glacier-proximal environment during the Younger Dryas and probably already during the Allerød. Sediment supply occurred from suspension fall out, ice rafting and mass-transport activity. The frequent colour changes from reddish brown to very dark greyish brown and very dark grey suggest sediment input from multiple sources. The general fining-upward trend (Fig. 2) is regarded to reflect the transition from a more glacier-proximal to a more distal environment. Predominantly higher percentages of angular IRD in unit I-Gs/interval IRD-6 (average 76%) are probably due to frequent iceberg rafting (Fig. 6; Table 4). However, peaks of more rounded grains (in particular within the interval between c. 768 and 822 cm in core JM98-845-PC) suggest periods of relatively increased sea-ice rafting and/or decreased iceberg rafting.

A clast-rich massive glacimarine diamicton (unit I-Gd/interval IRD-5) overlies the proximal glacimarine sediments (Figs. 2–4). It is characterised by high IRD flux and high percentages of angular IRD (Figs. 6–8; Table 4).

We suggest that the high IRD flux and the dominance of angular clasts in unit I-Gd are the result of intense iceberg rafting related to the final glacier withdrawal from Isfjorden to the inner parts of its tributaries, because 1) the unit is part of a continuous record linking Late Weichselian glacier-proximal sediments with the Holocene deposits, i.e. that it has to contain the final glacier withdrawal; 2) marked IRD peaks offshore western Svalbard are related to the Late Weichselian deglaciation (Mangerud et al., 1998; Ślubowska-Woldengen et al., 2007); 3) the general fining upward trend in the clay–silt–sand fractions (Fig. 2) is regarded as an indicator for an increasing distance to the sediment source.

The occasional occurrence of reddish brown, very dark greyish brown and very dark grey strata probably reflects a temporarily increased input from individual retreating glaciers surrounding Isfjorden.

The deposition of unit I-Gd terminated in the earliest Preboral, shortly prior to 9870 ± 65 ^{14}C BP (11,200 cal. years BP; Fig. 2; Table 3). This was the time when the deglaciation on Spitsbergen terminated and the glacier fronts had retreated to the fjord heads (e.g. Elverhøi et al., 1983; Mangerud et al., 1992; Elverhøi et al., 1995; Svendsen et al., 1996; Mangerud et al., 1998; Hald et al., 2004; Lønne, 2005).

The response of the glacier fronts on Spitsbergen to the Younger Dryas cooling is still debated. Whereas marked glacier-frontal deposits related to a Younger Dryas readvance are found in Scandinavia and Canada (e.g. Andersen et al., 1995; Lyså and Vorren, 1997; Dyke and Savelle, 2000; Vorren and Plassen, 2002), such morphological evidence is lacking on Spitsbergen. The low preservation potential of terrestrial deposits on Svalbard (Boulton et al., 1996; Lønne and Lyså, 2005) may account for this.

Retarded glacio-isostatic uplift (Forman et al., 1987; Landvik et al., 1987; Lehman and Forman, 1992) led Svendsen et al. (1996) to conclude that the glaciers in the inner parts of Isfjorden readvanced during the Younger Dryas cooling. It has been suggested that the tributaries of Isfjorden have been occupied by outlet glaciers and that their fronts were located either in the inner main fjord (Mangerud et al., 1992) or “far out in the main fjord” (Svendsen et al., 1996; see Fig. 1C).

A possible Younger Dryas readvance may be archived in the lithological units I-Gs and I-Gd.

The data from unit I-Gs do not provide any information about the IRD flux. However, the peaks of more rounded grains in the interval between c. 768 and 822 cm in core JM98-845-PC suggest a period of a relative increase in sea-ice rafting and/or decreased iceberg rafting (Fig. 6). This may reflect the Younger Dryas cooling and a related glacier readvance, because 1) glacier growth could have resulted in reduced iceberg calving; 2) reduced summer melt due to lower summer temperatures (compare with Birks et al., 1994) could have caused reduced iceberg calving during summer; 3) multi-annual and/or shorefast sea-ice suppressed the drift of icebergs across the core site.

High clay, as well as low silt and sand contents in this interval (Fig. 2) may point towards sedimentation mainly from suspension settling. This would support our suggestion that multi-annual and/or shorefast sea-ice suppressed iceberg rafting. The increasing percentages of angular grains and the coarsening in the topmost part of the

section may reflect periodic break-up of the sea ice and the onset of the glacier retreat following the Younger Dryas maximum ice extent.

Above, we argued that unit I-Gd was deposited during the final glacier withdrawal to the head of the tributaries of Isfjorden. However, because muddy diamictons with high clast contents occur in various glacimarine settings where high IRD flux reflects intensive iceberg calving related to the presence of ice streams, glacier advances or glacier retreats (Powell, 1984; Dowdeswell et al., 1994, 1998; Vorren and Plassen, 2002), it should not be excluded that an eventual Younger Dryas readvance is archived in this unit, in addition to the subsequent retreat.

Ślubowska-Woldengen et al. (2007) described only a slight increase in the IRD flux west off Svalbard during an early phase of the Younger Dryas. Koç et al. (2002) did not detect any significant IRD signal north off Svalbard during this period. Both observations may indicate that ice rafting was generally reduced during the cooling. This may exclude that unit I-Gd was deposited during the Younger Dryas. It could, however, support a potential increase sea-ice formation the interval between c. 768 and 822 cm in core JM98-845-PC as a consequence of the Younger Dryas cooling.

5.4. Holocene glacimarine environments

Clasts in unit I-M are suggested to reflect continuous ice rafting by sea ice and icebergs (Figs. 6, 8), implying that tidewater glaciers were present in the Isfjorden area throughout the entire Holocene. However, ice rafting has been significantly reduced compared to the Late Weichselian (Fig. 8).

Our suggestion is in contrast to observations by Svendsen and Mangerud (1997) who did not find any signs of Holocene glacial activity in Lake Linnévatnet after the Younger Dryas and prior to approximately 4000–5000 years BP, and in Billefjorden before c. 3000–4000 years BP. It supports, however, the results of Hald et al. (2004) from Van Mijenfjorden who found indications for a continuous presence of tidewater glaciers during the Holocene (for locations see Fig. 1).

Sub-unit I-Ml (intervals IRD-3, 4) was deposited between c. 11,200 and 9000 cal. years BP. The relatively low IRD flux (Fig. 8), but high amounts of paired shells, shell fragments and foraminifera are regarded to reflect the most favourable Holocene climatic and oceanographic conditions.

The period between c. 10,800 and 9700 cal. years BP was characterised by decreasing but oscillating IRD flux (Figs. 8, 9B–D). The generally decreasing IRD fluxes are suggested to reflect the ongoing general warming in the North Atlantic Region (Fig. 9E–G; Johnsen et al., 2001; Sarnthein et al., 2003; Hald et al., 2004). Peaks in the IRD flux generally resulted from synchronous increases in iceberg and sea-ice rafting prior to 10,200 cal. years BP (interval IRD-4). They were probably caused by short-lived synchronous climatic and oceanographic coolings in central Spitsbergen. These variations could have been related to short-lived atmospheric and oceanographic fluctuations on Greenland, the western Barents Sea and the continental slope off west Spitsbergen (Fig. 9E–G; Johnsen et al., 2001; Sarnthein et al., 2003; Hald et al., 2004).

After 10,200 cal. years BP, ice rafting occurred exclusively from icebergs (IRD-3; Figs. 8C, D; 9C, D). This change took place almost at the same time as the onset of the Holocene Thermal Optimum in the western Barents Sea and on the west Spitsbergen continental margin, lasting from c. 10,000 to c. 9000/8800 cal. years BP (Fig. 9E, F; Birks, 1991; Salvigsen et al., 1992; Sarnthein et al., 2003; Hald et al., 2004; Rasmussen et al., 2007). We assume that the formation of sea ice was significantly reduced or absent during this period, because 1) of the strong inflow of warm Atlantic Water to the western and northern Svalbard shelf, and its appearance as a surface-water mass off western Spitsbergen (Ślubowska-Woldengen et al., 2007; Rasmussen et al., 2007); 2) the mean July temperatures at the west coast of Spitsbergen were about 2 °C higher during the early Holocene than at present (Birks, 1991); 3) surface-water temperatures in west Spitsbergen fjords were 1–3 °C higher than at present (Salvigsen et al., 1992).

We assume that the iceberg-rafted debris originated from glaciers on east Spitsbergen, because glaciers along the west coast appear to have been absent at that time (Svendsen and Mangerud, 1997). This may point towards a strong east–west temperature gradient across Spitsbergen during the early Holocene.

The most favourable and stable environmental conditions during the Holocene in the western Barents Sea and Spitsbergen regions (Fig. 9E, F; this study, Sarnthein et al., 2003; Hald et al., 2004) occurred while the sea-surface conditions off Scandinavia were still generally unstable and influenced by the meltwater runoff from the Fennoscandian ice sheet (Klitgaard-Kristensen et al., 2001; Birks and Koç, 2002), and while Arctic conditions were still prevailing along a narrow zone over the western Greenland Basin (Koç et al., 1996). However, they occurred synchronously with the most favourable environmental conditions off north Iceland, in an area that presently is influenced by branches of the relatively warm Irminger Current (Fig. 1; Knudsen et al., 2004).

The early and synchronous timing for the Holocene Climatic Optimum off north Iceland, the western Barents Sea and the continental margin off west Spitsbergen (Sarnthein et al., 2003; Knudsen et al., 2004; Hald et al., 2004), as well as in Isfjorden is most probably the result of increased solar insolation and warmer Atlantic Water penetrating northwards (Fig. 9H; e.g. Berger and Loutre, 1991; Koç et al., 1993; Ślubowska-Woldengen et al., 2007). However, the fact that it precedes the Holocene Thermal Optimums in more central parts of the Nordic Seas with up to several thousand years (e.g. Harrison et al., 1992; Koç et al., 1993; Bauch et al., 2001; Duplessy et al., 2001; Johnsen et al., 2001; Klitgaard-Kristensen et al., 2001; Voronina et al., 2001; Birks and Koç, 2002; Nesje et al., 2005; Hald et al., 2007) can have several reasons. The ice sheets over Svalbard and the Barents Sea, as well as over Iceland, were significantly smaller and/or thinner than the ice sheets over Scandinavia and Greenland (e.g. Svendsen et al., 2004; Wohlfarth et al., 2008). This resulted in a rapid decay (compare with e.g. Landvik et al., 1998) and, in consequence, a rapidly decreasing influence on the climate and oceanography in these areas. Such a development opposes the situation in northwestern Europe where the ice sheets over Scandinavia and north America probably damped the effect of the high summer insolation until c. 8000 cal. years BP (e.g. Harrison et al., 1992; Duplessy et al., 2001; Nesje et al., 2005). Furthermore, a layer of relatively fresh water from these ice sheets might have restricted the warmer Atlantic Water masses to the subsurface (compare with Rasmussen et al., 2007) and, in consequence, limited the supply of heat to the atmosphere off northwestern Europe.

An increase in the IRD flux (Fig. 8), as well as lower amounts of shells, shell fragments and foraminifera in sub-unit I-Mu indicate generally cooler environmental conditions and an increase in glacial activity during the past c. 9000 cal. years BP. We distinguished the IRD intervals IRD-1 and 2, respectively (Figs. 6, 8; Table 4).

A period of increased iceberg rafting between c. 9000 and 8800 cal. years BP was followed by enhanced sea-ice rafting until approximately 8600 cal. years BP (Fig. 9C, D). The onset of iceberg rafting preceded a general cooling in the western Barents Sea and the Spitsbergen region, starting at c. 8800 cal. years BP (Fig. 9E, F; Birks, 1991; Wohlfarth et al., 1995; Sarnthein et al., 2003; Hald et al., 2004; Rasmussen et al., 2007). However, it correlated to a period of relatively large fluctuations in the $\delta^{18}O$ record, following a cold spell at c. 9300 cal. years BP on Greenland (Fig. 9G; Johnsen et al., 2001; Rasmussen et al., 2006; Vinther et al., 2006). The subsequent increase in sea-ice rafting occurred synchronously with a marked drop in sea-surface temperatures in the western Barents Sea and west off Spitsbergen (Fig. 9D-F; Sarnthein et al., 2003; Hald et al., 2004). These changes may reflect a sequence of marked environmental changes in the northernmost North Atlantic

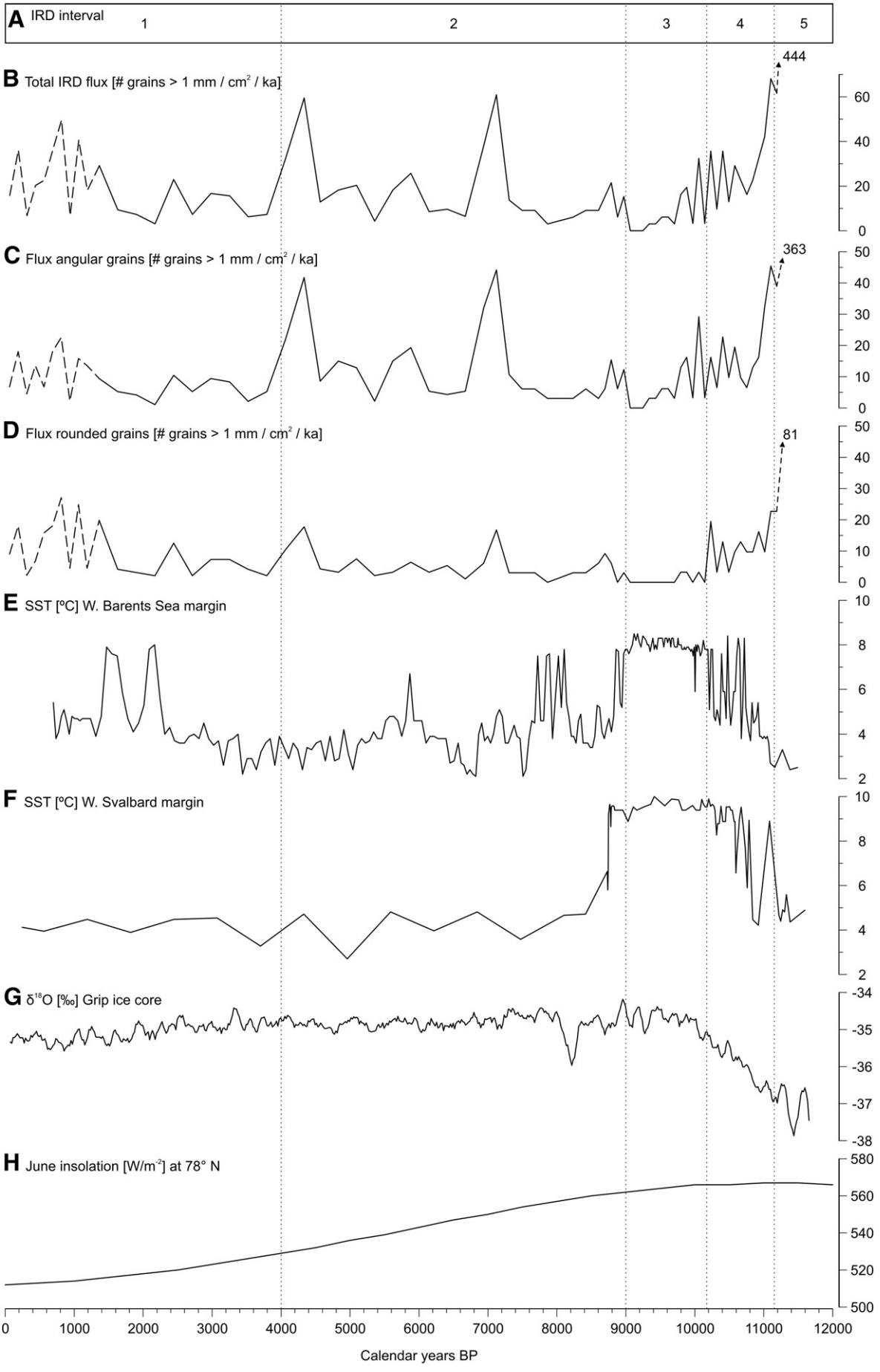
A IRD interval
1
2
3
4
5
B Total IRD flux [# grains > 1 mm / cm² / ka]
444
60
40
20
0
C Flux angular grains [# grains > 1 mm / cm² / ka]
363
50
40
30
20
10
0
D Flux rounded grains [# grains > 1 mm / cm² / ka]
81
50
40
30
20
10
0
E SST [°C] W. Barents Sea margin
10
8
6
4
2
F SST [°C] W. Svalbard margin
10
8
6
4
2
G δ18O [‰] Grip ice core
-34
-35
-36
-37
-38
H June insolation [W/m-2] at 78° N
580
560
540
520
500
0
1000
2000
3000
4000
5000
6000
7000
8000
9000
10000
11000
12000
Calendar years BP

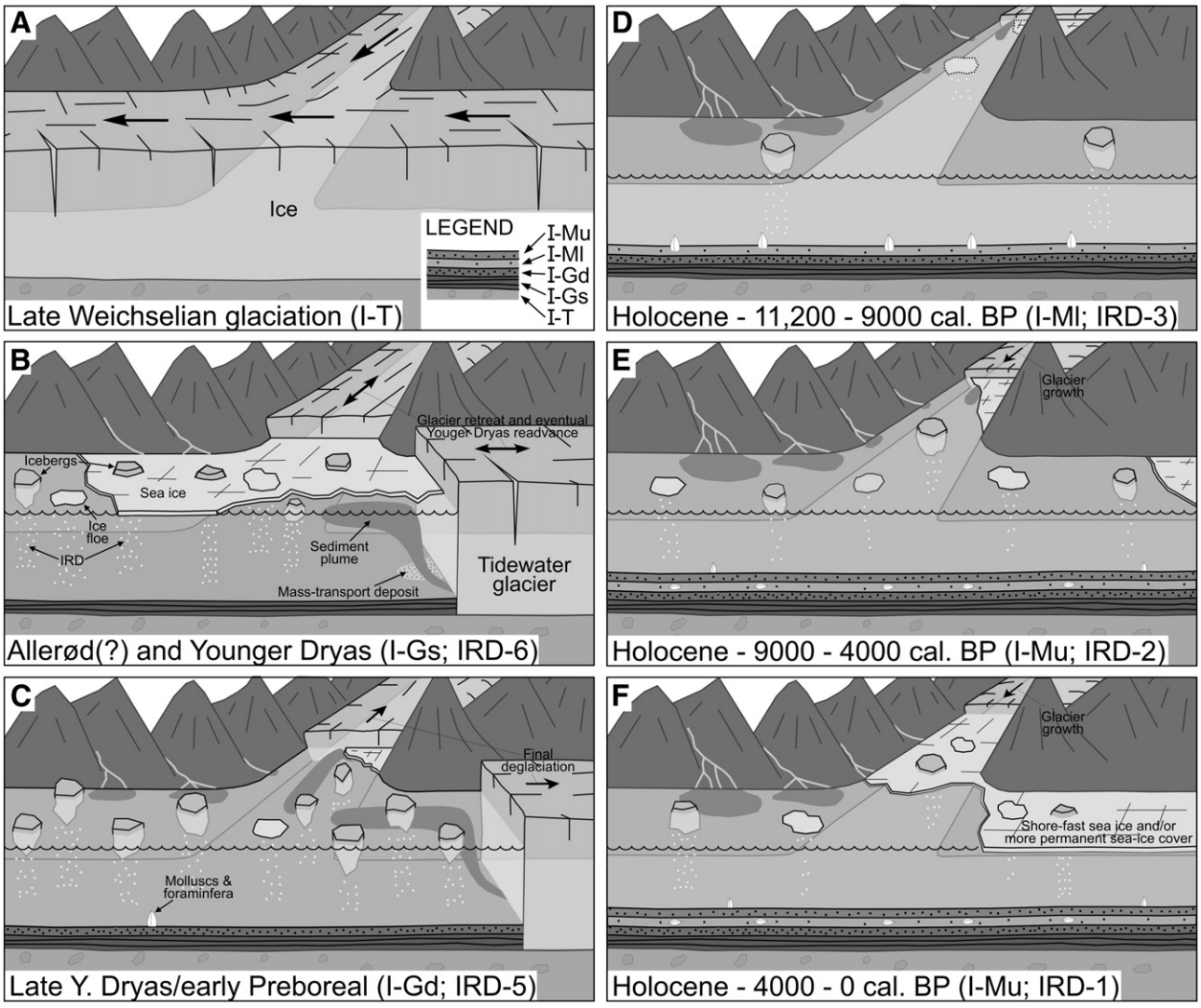

Fig. 10. Summary of the sedimentary processes and glacial activity in the Isfjorden area from the Late Weichselian glaciations until the present. The dashed lines on Fig. D indicate decreasing sea-ice rafting during this period.

commencing with a marked cooling on Greenland c. 9300 cal. years BP (Johnsen et al., 2001). This might have led to decreasing air temperatures and/or increased precipitation on Spitsbergen, resulting in glacier growth and increased iceberg calving latest around 9000 cal. years BP (note that this is a minimum age, because some ice rafting occurred between c. 9300 and 9000 cal. years BP — see Section 4.5.2). The subsequent decrease in iceberg rafting and enhanced sea-ice rafting might indicate that a 'cooling threshold' was crossed, leading to a marked drop in sea-surface temperatures in the Svalbard–Barents Sea region at c. 8800 cal. years BP (Fig. 9E, F; Sarnthein et al., 2003; Hald et al., 2004). The low temperatures might have resulted in glacier growth without iceberg calving. The comparison of our results with other data (Fig. 9; Johnsen et al., 2001; Sarnthein et al., 2003; Hald et al., 2004; Rasmussen et al., 2006; Vinther et al., 2006) indicates that Spitsbergen fjords are settings that can archive asynchronous atmospheric and oceanographic environmental variations in the European Arctic.

The fluctuating and comparatively high IRD fluxes between c. 9000 and 4000 cal. years BP (interval IRD-2; Figs. 8, 9B—D) are suggested to be related to the cooling in the Svalbard–Barents Sea region (Birks, 1991; Wohlfarth et al., 1995; Sarnthein et al., 2003; Hald et al., 2004; Rasmussen et al., 2007). The onset of the cooling in this region correlates comparatively well with the onset of a cooling off north Iceland starting at c. 9000 cal. BP (Knudsen et al., 2004). However, it started before large areas in and around the Nordic Seas had reached their most favourable Holocene environmental conditions, because these were still affected by the ongoing meltdown of the Fennoscandian, Laurentide and Greenland ice sheets (e.g. Harrison et al., 1992; Koç et al., 1993; Bauch et al., 2001; Duplessy et al., 2001; Johnsen et al., 2001; Klitgaard–Kristensen et al., 2001; Voronina et al., 2001; Birks and Koç, 2002; Calvo et al., 2002; Nesje et al., 2005; Hald et al., 2007).

The ice rafting in central Isfjorden during this time occurred mainly from icebergs (Fig. 9C, D). Short-lasting increases in the flux of iceberg-rafted debris may have been caused by 1) less sea-ice cover during temporal warming or intrusions of warmer water masses into Isfjorden, allowing more icebergs to drift across the core site, 2) increased iceberg rafting related to glacier surges, or 3) random dumping from icebergs.

However, because the fluctuations in iceberg rafting mostly correlate with fluctuations in sea-ice rafting, we assume that these are the result of synchronous climatic and oceanographic variations. Whether these variations are coolings or warmings cannot be inferred from our data. They indicate at least that open waters must have

Fig. 9. Correlation of results from this study (A–D) with (E) sea-surface temperatures in the western Barents Sea (Sarnthein et al., 2003), (F) sea-surface temperatures off western Svalbard (Hald et al., 2004), (G) $\delta^{18}O$ measurements from the Grip ice core (Rasmussen et al., 2006; Vinther et al., 2006) and (H) June insolation at 78°N(Berger and Loutre, 1991).

existed temporarily, allowing relatively large amounts of icebergs and sea ice to drift across the core site.

The peak flux of angular grains around 5800 cal. years BP correlates to a temporal sea-surface temperature increase in the western Barents Sea (Fig. 9E; Sarnthein et al., 2003). Since no increase in the sea-ice flux occurs, we suggest that this peak reflects a period of stronger inflow of warmer waters into the Isfjorden area, suppressing the formation of sea ice and enhancing iceberg calving. The subsequent drop in iceberg calving occurred simultaneously with a temperature decrease in the western Barents Sea and probably reflects another glacier growth where more ice is retained in the glaciers.

As previously mentioned, the ice caps covering Svalbard and the Barents Sea decayed rapidly at the end of the last glaciation (Landvik et al., 1998), resulting in a very reduced influence on the environment in the western Barents Sea-Svalbard region. Therefore, we assume that the cooling starting around c. 9000 cal. BP was mainly driven by decreasing solar insolation and the related decrease in heat flux to the high northern latitudes (Fig. 9H; Berger and Loutre, 1991; Hald et al., 2004; Ślubowska et al., 2005; Hald et al., 2007).

A general decrease in the IRD flux occurred around 4000 cal. years BP (interval IRD-1; Figs. 8, 9B–D; Table 4). From then, and at least until 1300 cal. years BP, ice rafting took place to almost equal proportions from icebergs and sea ice. The decrease in IRD flux is probably the result of the enhanced formation of shore-fast sea ice and/or more permanent sea-ice cover that generally reduced the drift of sea ice and icebergs in central Isfjorden. We assume that the reduced iceberg rafting reflects conditions where icebergs were trapped and forced to release their debris close to the calving fronts in the tributaries of Isfjorden (compare with Ó Cofaigh and Dowdeswell, 2001). This enhanced formation of sea ice is most probably the consequence of decreasing heat flux along the western Scandinavian–Svalbard margin related to the cooling in the entire north Atlantic region (e.g. Birks, 1991; Koç et al., 1993; Svendsen and Mangerud, 1997; Klitgaard-Kristensen et al., 2001; Voronina et al., 2001; Hald et al., 2004; Nesje et al., 2005; Rasmussen et al., 2007; Ślubowska-Woldengen et al., 2007).

6. Conclusions

1. A basal till in central Isfjorden was deposited beneath an ice stream prior to 12,700 cal. years BP (Fig. 10A). Some of the material was transported at least 50 km.
2. Proximal glacimarine conditions, that were influenced by several tidewater glaciers, prevailed during most of the Younger Dryas and probably already during the Allerød (Fig. 10B). Ice rafting occurred mainly from icebergs. The Younger Dryas cooling might be reflected by increased sea-ice formation and reduced iceberg rafting, in addition to a relative increase in suspension settling.
3. Iceberg rafting dominated the final deglaciation that terminated around 11,200 cal. years BP (Fig. 10C).
4. The most favourable Holocene climatic and oceanographic conditions occurred between c. 11,200 and 9000 cal. years BP (Fig. 10D). They were probably the result of high solar insolation and enhanced oceanic heat flux. Ice rafting decreased significantly and occurred almost exclusively from icebergs after 10,200 years BP. The icebergs were most probably released from remaining ice masses on east Spitsbergen, suggesting the presence of a strong east–west temperature gradient on Spitsbergen during this time.
5. Generally enhanced ice rafting between 9000 and 4000 cal. years BP (Fig. 10E) is related to atmospheric and oceanographic cooling in the western Barents Sea–Svalbard region, as the result of decreased solar insolation and oceanic heat flux. The cooling period commenced with an increase in iceberg rafting between c. 9000 and 8800 cal. years BP, followed by an increase in sea-ice rafting until approximately 8600 cal. years BP.
6. Decreasing ice rafting after 4000 cal. years BP is regarded to be the result of the ongoing cooling. It most probably reflects the enhanced formation of shore-fast and/or more permanent sea-ice cover, reducing the drift of icebergs and sea ice in the Isfjorden area (Fig. 10F).
7. The sedimentary record in central Isfjorden reveals that the palaeoenvironmental conditions on central Spitsbergen mainly correlate with the oceanographic conditions in the western Barents Sea and the shelf off western Svalbard. However, it also shows that climatic and oceanographic changes on Greenland and in the entire north Atlantic region can have an impact on the environment on Spitsbergen.

Acknowledgements

This study was performed as part of the Strategic University Programme SPONCOM (Sedimentary Processes and Palaeoenvironment on Northern Continental Margins), financed by the Research Council of Norway. The masters and crews of *R/V Jan Mayen* supported the data collection. Steinar Iversen provided technical help during and after the cruises. Jan P. Holm helped with several figures. Edel Ellingsen, Trine Dahl, Elsebeth Thomsen and Henrik Rasmussen supported the laboratory analyses. The Roald Amundsen Centre for Arctic Research at the University of Tromsø provided funding for the radiocarbon dates. Jan Sverre Laberg gave constructive comments on an earlier draft of the manuscript. Editor in chief Thierry Corrège, Jochen Knies and one anonymous reviewer critically reviewed the manuscript and provided constructive comments for improvements. We extend our most sincere thanks to these persons and institutions.

References

Alley, R.B., Blankenship, D.D., Bentley, C.R., Rooney, S.T., 1986. Deformation of till beneath ice stream B, West Antarctica. Nature 322, 57–59.
Andersen, B.G., Mangerud, J., Sørensen, R., Reite, A., Sveian, H., Thoresen, M., Bergström, B., 1995. Younger Dryas ice-marginal deposits in Norway. Quaternary International 28, 147–169.
Bauch, H.A., Erlenkeuser, H., Spielhagen, R.F., Struck, U., Matthiessen, J., Thiede, J., Heinemeier, J., 2001. A multiproxy reconstruction of the evolution of deep and surface water in the subarctic Nordic seas over the last 30,000 yr. Quaternary Science Reviews 20, 659–678.
Benn, D.I., Evans, D.J.A., 1996. The interpretation and classification of subglacially-deformed materials. Quaternary Science Reviews 15, 23–52.
Berger, A., Loutre, M.F., 1991. Insolation values for the climate of the last 10 million years. Quaternary Science Reviews 10, 297–317.
Birks, H.H., 1991. Holocene vegetational history and climatic change in west Spitsbergen — plant macrofossils from Skardtjørna, an Arctic late. Holocene 1, 209–218.
Birks, C.J.A., Koç, N., 2002. A high-resolution diatom record of late-Quaternary sea-surface temperatures and oceanographic conditions from the eastern Norwegian Sea. Boreas 31, 323–344.
Birks, H.H., Paus, A., Svendsen, J.I., Alm, T., Mangerud, J., Landvik, J.Y., 1994. Late Weichselian environmental change in Norway, including Svalbard. Journal of Quaternary Science 9, 133–145.
Boulton, G.S., 1979. Glacial history of the Spitsbergen archipelago and the problem of a Barents Shelf ice sheet. Boreas 8, 31–57.
Boulton, G.S., van der Meer, J.J.M., Hart, J., Beets, D., Ruegg, G.H.J., van der Wateren, F.M., Jarvis, J., 1996. Till and moraine emplacement in a deforming bed surge — an example from a marine environment. Quaternary Science Reviews 15, 961–987.
Cortese, G., Dolven, J.K., Bjørklund, K.R., Malmgren, B.A., 2005. Late Pleistocene–Holocene radiolarian paleotemperatures in the Norwegian Sea based on artificial neural networks. Palaeogeography, Palaeoclimatology, Palaeoecology 224, 311–332.
Cottier, F.R., Nilsen, F., Inall, M.E., Gerland, S., Tverberg, V., Svendsen, H., 2007. Wintertime warming of an Arctic shelf in response to large-scale atmospheric circulation. Geophysical Research Letters 34. doi:10.1029/2007/GL029948.
Dallmann, W.K., Ohta, Y., Elvevold, S., Blomeier, D., 2002. Bedrock map of Svalbard and Jan Mayen. Norsk Polarinstitutt Temakart No. 33.
Dowdeswell, J.A., Whittington, R.J., Marienfeld, P., 1994. The origin of massive diamicton facies by iceberg rafting and scouring, Scoresby Sund, East Greenland. Sedimentology 41, 21–35.
Dowdeswell, J.A., Elverhøi, A., Spielhagen, R., 1998. Glacimarine sedimentary processes and facies on the polar North Atlantic margins. Quaternary Science Reviews 17, 243–272.
Duplessy, J.-C., Ivanova, E., Murdmaa, I., Paterne, M., Laberyie, L., 2001. Holocene paleoceanography of the northern Barents Sea and variations of the northward heat transport by the Atlantic Ocean. Boreas 30, 2–16.
Dyke, A.S., Savelle, J.M., 2000. Major end moraines of Younger Dryas age on Wollaston Peninsula, Victoria Island, Canadian Arctic: implications for paleoclimate and for formation of hummocky moraine. Canadian Journal of Earth Sciences 37, 601–619.

Elverhøi, A., Lønne, Ø., Seland, R., 1983. Glaciomarine sedimentation in a modern fjord environment, Spitsbergen. Polar Research 1, 127–149.
Elverhøi, A., Svendsen, J.I., Solheim, A., Andersen, E.S., Milliman, J., Mangerud, J., Hooke, R.LeB, 1995. Late Quaternary Sediment Yield from the High Arctic Svalbard Area. Journal of Geology 103, 1–17.
Forman, S.L., Mann, D.H., Miller, G.H., 1987. Late Weichselian and Holocene relative sea-level history of Bröggerhalvöya. Quaternary Research 27, 41–50.
Forwick, M., Vorren, T.O., 2007. Holocene mass-transport activity and climate in outer Isfjorden, Spitsbergen: marine and subsurface evidence. Holocene 17, 707–716.
Gilbert, R., 1990. Rafting in glacimarine environments. In: Dowdeswell, J.A., Scourse, J.D. (Eds.), Glacimarine Environments: Processes and Sediments. Geological Society Special Publication No 53, pp. 105–120.
Goldschmidt, P.M., Pfirman, S.L., Wollenburg, I., Henrich, R., 1992. Origin of sediment pellets from the Arctic seafloor: sea ice or icebergs? Deep-Sea Research 39, S539–S565.
Hagen, J.O., Liestøl, O., Roland, E., Jørgensen, T., 1993. Glacier atlas of Svalbard and Jan Mayen. Norsk Polarinstitutt Meddelelser, vol. 129. 141 pp.
Hald, M., Hagen, S., 1998. Early Preboreal cooling in the Nordic seas region triggered by meltwater. Geology 26, 615–618.
Hald, M., Korsun, S., 2008. The 8200 cal. yr BP event reflected in the Arctic fjord, Van Mijenfjorden, Svalbard. Holocene 18, 981–990.
Hald, M., Kolstad, V., Polyak, L., Forman, S.L., Herlihy, F.A., Ivanov, G., Nescheretov, A., 1999. Late-glacial and Holocene paleoceanography and sedimentary environments in the St. Anna Trough, Eurasian Arctic Ocean margin. Palaeogeography, Palaeoclimatology, Palaeoecology 146, 229–249.
Hald, M., Ebbesen, H., Forwick, M., Godtliebsen, F., Khomenko, L., Korsun, S., Ringstad Olsen, L., Vorren, T.O., 2004. Holocene paleoceanography and glacial history of the West Spitsbergen area, Euro-Arctic margin. Quaternary Science Reviews 23, 2075–2088.
Hald, M., Andersson, C., Ebbesen, H., Jansen, E., Klitgaard-Kristensen, D., Risebrobakken, B., Salomonsen, G.R., Sarnthein, M., Sejrup, H.P., Telford, R.J., 2007. Variations in temperature and extent of Atlantic Water in the northern North Atlantic during the Holocene. Quaternary Science Reviews 26, 3423–3440.
Hansbo, S., 1957. A new approach to determination of the shear strength of clay by the fallcone test. Royal Swedish Geotechnical Institute Proceedings, vol. 14. 47 pp.
Harrison, S.P., Prentice, I.C., Bartlein, P.J., 1992. Influence of insolation and glaciation on atmospheric circulation in the North Atlantic sector: implications of general circulation model experiments for the Late Quaternary climatology in Europe. Quaternary Science Reviews 11, 283–299.
Hooke, R.LeB, Elverhøi, A., 1996. Sediment flux from a fjord during glacial periods, Isfjorden, Spitsbergen. Global and Planetary Change 12, 237–249.
Hughen, K.A., Baillie, M.G.L., Bard, E., Bayliss, A., Beck, J.W., Bertrand, C., Blackwell, P.G., Buck, C.E., Burr, G., Cutler, K.B., Damon, P.E., Edwards, R.L., Fairbanks, R.G., Friedrich, M., Guilderson, T.P., Kromer, B., McCorman, F.G., Manning, S., Bronk Ramsey, C., Reimer, P.J., Reimer, R.W., Remmele, S., Southon, J.R., Stuiver, M., Talamo, S., Taylor, F.W., van der Plicht, J., Weyhenmeyer, C.E., 2004. Marine04 Marine radiocarbon age calibration, 26–0 ka BP. Radiocarbon 46, 1059–1086.
IPCC, 2007. Summary for Policymakers. In: Solomon, S., Qin, D., Manning, M., Chen, Z., Marquis, M., Averyt, K.B., Tignor, M., Miller, H.L. (Eds.), Climate Change 2007: The Physical Science Basis Contribution of Working Group I to the Fourth Assessment Report of the Intergovernmental Panel on Climate Change. InCambridge University Press, Cambridge, United Kingdom and New York, NY, USA.
Isaksson, E., Hermanson, M., Hicks, S., Igarashi, M., Kamiyama, K., Moore, J., Motoyama, H., Muir, D., Pohjola, V., Vaikmäe, R., van de Wal, R.S.W., Watanabe, O., 2003. Ice cores from Svalbard — useful archives of past climate and pollution history. Physics and Chemistry of the Earth 28, 1217–1228.
Isaksson, E., Kohler, J., Pohjola, V., Moore, J., Igarashi, M., Karlöf, L., Martma, T., Meijer, H., Motoyama, H., Vaikmäe, R., van de Wal, R.S.W., 2005. Two ice-core $\delta^{18}O$ records from Svalbard illustrating climate and sea-ice variability over the last 400 years. Holocene 15, 501–509.
Johnsen, S.J., Dahl-Jensen, D., Gundestrup, N., Steffensen, J.P., Clausen, H.B., Miller, H., Masson-Delmotte, V., Sveinbjörnsdottir, A.E., White, J., 2001. Oxygen isotope and palaeotemperature records from six Greenland ice-core stations: Camp Century, Dye-3, GRIP, GISP2, Renland and NorthGrip. Journal of Quaternary Science 16, 299–307.
Klitgaard-Kristensen, D., Sejrup, H.P., Haflidason, H., 2001. The last 18 kyr fluctuations in Norwegian Sea surface conditions and implications for the magnitude of climatic change: evidence from the North Sea. Paleoceanography 16, 455–467.
Knies, J., Kleiber, H.-P., Matthiessen, J., Müller, C., Nowaczyk, N., 2001. Marine ice-rafted debris records constrain maximum extent of Saalian and Weichselian ice-sheets along the northern Eurasian margin. Global and Planetary Change 31, 45–64.
Knudsen, K.L., Jiang, H., Jansen, E., Eiríksson, J., Heinemeier, J., Seidenkrantz, M.-S., 2004. Environmental changes off North Iceland during the deglaciation and the Holocene: foraminifera, diatoms and stable isotopes. Marine Micropaleontology 50, 273–305.
Koç, N., Jansen, E., 1994. Response of the high-latitude Northern Hemisphere to orbital climate forcing: evidence from the Nordic Seas. Geology 22, 523–526.
Koç, N., Jansen, E., Haflidason, H., 1993. Paleoceanographic reconstructions of surface ocean conditions in the Greenland, Iceland and Norwegian sea through the last 14 ka based on diatoms. Quaternary Science Reviews 12, 115–140.
Koç, N., Jansen, E., Hald, M., Labeyrie, L., 1996. Late glacial–Holocene sea surface temperatures and gradients between the North Atlantic and the Norwegian Sea: implications for the Nordic heat pump. In: Andrews, J.T., Austin, W.E.N., Bergsten, H., Jennings, A.E. (Eds.), Late Quaternary Palaeoceanography of the North Atlantic Margins: Geological Society Special Publications, vol. 111, pp. 177–185.
Koç, N., Klitgaard-Kristensen, D., Hasle, K., Forsberg, C.F., Solheim, A., 2002. Late glacial palaeoceanography of Hinlopen Strait, northern Svalbard. Polar Research 21m, 307–314.
Landvik, J.Y., Mangerud, J., Salvigsen, O., 1987. The Late Weichselian and Holocene shoreline displacement on the west-central coast of Svalbard. Polar Research 5, 29–44.
Landvik, J.Y., Bondevik, S., Elverhøi, A., Fjeldskaar, W., Mangerud, J., Salvigsen, O., Siegert, M.J., Svendsen, J.-I., Vorren, T.O., 1998. The last glacial maximum of Svalbard and the Barents Sea area: ice sheet extent and configuration. Quaternary Science Reviews 17, 43–75.
Landvik, J.Y., Ingólfsson, Ó., Mienert, J., Lehman, S.J., Solheim, A., Elverhøi, A., Ottesen, D., 2005. Rethinking Late Weichselian ice sheet dynamics in coastal NW Svalbard. Boreas 34, 7–24.
Lehman, S.J., Forman, S.L., 1992. Late Weichselian glacier retreat in Kongsfjorden, West Spitsbergen, Svalbard. Quaternary Research 37, 139–154.
Lisitzin, A.P., 2002. Sea-Ice and Iceberg Sedimentation in the Ocean — Recent and Past. Springer-Verlag. 563 pp.
Lønne, I., 2005. Faint traces of high Arctic glaciations: an early Holocene ice-front fluctuation in Bolterdalen, Svalbard. Boreas 34, 308–323.
Lønne, I., Lysså, A., 2005. Deglaciation dynamics following the Little Ice Age on Svalbard: implications for shaping of landscapes at high latitudes. Geomorphology 72, 300–319.
Lubinski, D.J., Polyak, L., Forman, S.L., 2001. Freshwater and Atlantic water inflows to the deep northern Barents and Kara seas since ca. 13 ^{14}C ka: foraminifera and stable isotopes. Quaternary Science Reviews 20, 1851–1879.
Lysså, A., Vorren, T.O., 1997. Seismic facies and architecture of ice-contact submarine fans in high-relief fjords, Tromsø, Northern Norway. Boreas 26, 309–328.
Mackiewicz, N.E., Powell, R.D., Carlson, P.R., Molnia, B.F., 1984. Interlaminated ice-proximal glacimarine sediments in Muir Inlet, Alaska. Marine Geology 57, 113–147.
Majewski, W., Zajączkowski, M., 2007. Benthic foraminifera in Adventfjorden, Svalbard: Last 50 years of local hydrographic changes. Journal of Foraminiferal Research 37, 107–124.
Majewski, W., Szczuciński, W., Zajączkowski, M., 2009. Interactions of Arctic and Atlantic water-masses and associated environmental changes during the last millennium, Hornsund (SW Svalbard). Boreas. doi:10.1111/j.1502-3885.2009.00091.x.
Mangerud, J., Gulliksen, S., 1975. Apparent radiocarbon ages of recent marine shells from Norway, Spitsbergen, and Arctic Canada. Quaternary Research 5, 263–273.
Mangerud, J., Svendsen, J.I., 1990. Deglaciation chronology inferred from marine sediments in a proglacial lake basein, western Spitsbergen, Svalbard. Boreas 19, 249–272.
Mangerud, J., Landvik, J., 2007. Younger Dryas cirque glaciers in western Spitsbergen: smaller than during the Little Ice Age. Boreas 36, 278–285.
Mangerud, J., Bolstad, M., Elgersma, A., Helliksen, D., Landvik, J.Y., Lønne, I., Lycke, A.K., Salvigsen, O., Sandahl, T., Svendsen, J.I., 1992. The Last Glacial Maximum on Spitsbergen. Quaternary Research 38, 1–31.
Mangerud, J., Dokken, T., Hebbeln, D., Heggen, B., Ingólfsson, Ó., Landvik, J.Y., Mejdahl, V., Svendsen, J.I., Vorren, T.O., 1998. Fluctuations of the Svalbard–Barents Sea ice sheet during the last 150 000 years. Quaternary Science Reviews 17, 11–42.
Moros, M., Emeis, K., Risebrobakken, B., Snowball, I., Kuijpers, A., McManus, J., Jansen, E., 2004. Sea surface temperatures and ice rafting in the Holocene North Atlantic: climate influences on northern Europe and Greenland. Quaternary Science Reviews 23, 2113–2126.
Nesje, A., Dahl, S.O., Bakke, J., 2004. Were abrupt Lateglacial and early–Holocene climatic changes in northwest Europe linked to freshwater outbursts to the North Atlantic and Arctic Oceans? Holocene 14, 299–310.
Nesje, A., Bakke, J., Dahl, S.O., Lie, Ø., Matthews, J.A., 2008. Norwegian mountain glaciers in the past, present and future. Global and Planetary Change 60, 10–27.
Nesje, A., Jansen, E., Birks, H.J.B., Bjune, A.E., Bakke, J., Andersson, C., Dahl, S.O., Klitgaard Kristensen, D., Lauritzen, S.-E., Lie, Ø., Risebrobakken, B., Svendsen, J.I., 2005. Holocene climate variability in the Northern North Atlantic Region: a review of terrestrial and marine evidence. In: Drange, H., Dokken, T., Furevik, T., Gerdes, R., Berger, W. (Eds.), The Nordic seas: an integrated perspective. geophysical monograph. In: Geophysical Monograph Series, vol. 158. American Geophysical Union, Washington, DC, pp. 289–322.
Nilsen, F., Cottier, F., Skogseth, R., Mattsson, S., 2008. Fjord-shelf exchanges controlled by ice and brine production: the interannual variation of Atlantic Water in Isfjorden, Svalbard. Continental Shelf Research 28, 1838–1853.
Ó Cofaigh, C., Dowdeswell, J.A., 2001. Laminated sediments in glacimarine environments: diagnostic criteria for their interpretation. Quaternary Science Reviews 20, 1411–1436.
Ottesen, D., Dowdeswell, J.A., Rise, L., 2005. Submarine landforms and the reconstruction of fast-flowing ice streams within a large Quaternary ice sheet: the 2500-km-long Norwegian-Svalbard margin (57–80 N). Geological Society of America Bulletin 117, 1033–1050.
Powell, R.D., 1984. Glacimarine processes and inductive lithofacies modelling of ice shelf and tidewater glacier sediments based on Quaternary examples. Marine Geology 57, 1–52.
Powell, R.D., Molnia, B.F., 1989. Glacimarine sedimentary processes, facies and morphology of the south-southeast Alaska shelf and fjords. Marine Geology 85, 359–390.
Rasmussen, S.O., Andersen, K.K., Svensson, A.M., Steffensen, J.P., Vinther, B.M., Clausen, H.B., Siggaard-Andersen, M.-L., Johnsen, S.J., Larsen, L.B., Dahl-Jensen, D., Bigler, M., Röthlisberger, R., Fischer, H., Goto-Azuma, K., Hansson, M.E., Ruth, U., 2006. A new Greenland ice core chronology for the last glacial termination. Journal of Geophysical Research 111. doi:10.1029/2005JD006079.

Rasmussen, T.L., Thomsen, E., Ślubowska, M.A., Jessen, S., Solheim, A., Koç, N., 2007. Paleoceanographic evolution of the SW Svalbard margin (76 N) since 20,000 ^{14}C yr BP. Quaternary Research 67, 100–114.

Renssen, H., Goose, H., Fichefet, T., Brovkin, V., Driesschaert, E., Wolk, F., 2005. Simulating the Holocene climate evolution at northern high latitudes using a coupled atmosphere-sea ice-ocean-vegetation model. Climate Dynamics 24, 23–43.

Rohling, E.J., Pälike, H., 2005. Centennial-scale climate cooling with a sudden cold event around 8, 200 years ago. Nature 434, 975–979.

Saloranta, T.M., Haugan, P.M., 2004. Northward cooling and freshening of the warm core of the West Spitsbergen Current. Polar Research 23, 79–88.

Salvigsen, O., Forman, S.L., Miller, G.H., 1992. Thermophilus molluscs on Svalbard during the Holocene and their paleoclimatic implications. Polar Research 11, 1–10.

Sarnthein, M., Van Kreveld, S., Erlenkeuser, H., Grootes, P.M., Kucera, M., Plaumann, U., Schulz, M., 2003. Centennial-to-millennial-scale periodicities of Holocene climate and sediment injections off the western Barents shelf 75 N. Boreas 32, 447–461.

Schauer, U., Fahrbach, E., Osterhus, S., Rohardt, G., 2004. Arctic warming through the Fram Strait: Oceanic heat transport from 3 years of measurements. Journal of Geophysical Reaseach 109. doi:10.1029/2003JC001823.

Ślubowska, M.A., Koç, N., Rasmussen, T.L., Klitgaard-Kristensen, D., 2005. Changes in the flow of Atlantic water into the Arctic Ocean since the last deglaciation: evidence from the northern Svalbard continental margin, 80ºN. Paleoceanography 20. doi:10.1029/2005PA001141.

Ślubowska-Woldengen, M., Rasmussen, T.L., Koç, N., Klitgaard-Kristensen, D., Nilsen, F., Solheim, A., 2007. Advection of Atlantic Water to the western and northern Svalbard shelf since 17, 500 cal yr BP. Quaternary Science Reviews 26, 463–478.

Ślubowska-Woldengen, M., Koç, N., Rasmussen, T.L., Klitgaard-Kristensen, D., Hald, M., Jennings, A.E., 2008. Time-slice reconstructions of ocean circulation changes on the continental shelf in the Nordic and Barents Seas during the last 16,000 cal yr B.P.

Stuiver, M., Reimer, P.J., 1993. Extended ^{14}C database and revised CALIB radiocarbon calibration program. Radiocarbon 35, 215–230.

Svendsen, J.I., Mangerud, J., 1992. Paleoclimatic inferences from glacial fluctuations on Svalbard during the last 20 000 years. Climate Dynamics 6, 213–220.

Svendsen, J.I., Mangerud, J., 1997. Holocene glacial and climatic variations on Spitsbergen, Svalbard. Holocene 7, 45–57.

Svendsen, H., Beszczynska-Møller, A., Hagen, J.O., Lefauconnier, B., Tverberg, V., Gerland, S., Ørbæk, J.B., Bischof, K., Papucci, C., Zajaczkowski, M., Azzolini, R., Bruland, O., Wiencke, C., Winther, J.-G., Dallmann, W., 2002. The physical environment of Kongsfjorden-Krossfjorden, an Arctic fjord system in Svalbard. Polar Research 21, 133–166.

Svendsen, J.I., Mangerud, J., Elverhøi, A., Solheim, A., Schüttenhelm, R.T.E., 1992. The Late Weichselian glacial maximum on western Spitsbergen inferred from offshore sediment cores. Marine Geology 104, 1–17.

Svendsen, J.I., Elverhøi, A., Mangerud, J., 1996. The retreat of the Barents Sea Ice Sheet on the western Svalbard margin. Boreas 25, 244–256.

Svendsen, J.I., Alexanderson, H., Astakhov, V.I., Demidov, I., Dowdeswell, J.A., Funder, S., Gataullin, V., Henriksen, M., Hjort, C., Houmark-Nielsen, M., Hubberten, H.W., Ingólfsson, Ó., Jakobsson, M., Kjær, K.H., Larsen, E., Lokrantz, H., Lunkka, J.P., Lyså, A., Mangerud, J., Matiouchkov, A., Murray, A., Möller, P., Niessen, F., Nikolskaya, O., Polyak, L., Sarrnisto, M., Siegert, C., Siegert, M.J., Spielhagen, R.F., Stein, R., 2004. Late Quaternary ice sheet history of northern Eurasia. Quaternary Science Reviews 23, 1229–1271.

Vinther, B.M., Clausen, H.B., Johnsen, S.J., Rasmussen, S.O., Andersen, K.K., Buchardt, S.L., Dahl-Jensen, D., Seierstad, I.K., Siggaard-Andersen, M.-L., Steffensen, J.P., Svensson, A., Olsen, J., Heinemeier, J., 2006. A synchronized dating of three Greenland ice cores throughout the Holocene. Journal of Geophysical Research 111. doi:10.1029/2005JD006921.

Voronina, E., Polyak, L., de Vernal, A., Peyron, O., 2001. Holocene variations of sea-surface conditions in the southeastern Barents Sea, reconstructed from dino-flaggelate cyst assemblages. Journal of Quaternary Science 16, 717–726.

Vorren, T.O., Plassen, L., 2002. Deglaciation and palaeoclimate of the Andfjord–Vågsfjord area, north Norway. Boreas 31, 97–125.

Werner, A., 1993. Holocene moraine chronology, Spitsbergen, Svalbard: lichenometric evidence for multiple Neoglacial advances in the Arctic. Holocene 3, 128–137.

Węsławski, J.M., Koszteyn, J., Zajaczkowski, M., Wiktor, J., Kwaśniewski, S., 1995. Fresh water in Svalbard fjord ecosystems. In: Skjoldal, H.R., Hopkins, C., Erikstad, K.E., Leinaa, H.P. (Eds.), Ecology of Fjords and Coastal Waters, pp. 229–241.

Wohlfarth, B., Lemdahl, G., Olsson, S., Persson, T., Snowball, I., Ising, J., Jones, V., 1995. Early Holocene environment on Bjørnøya (Svalbard) inferred from multidisciplinary lake sediment studies. Polar Research 14, 253–275.

Wohlfarth, B., Björck, S., Funder, S., Houmark-Nielsen, M., Ingólfsson, Ó., Lunkka, J.-P., Mangerud, J., Saarnisto, M., Vorren, T.O., 2008. Quaternary of Norden. Episodes 31, 73–81.

Zajączkowski, M., Szczuciński, W., Bojanowski, R., 2004. Recent changes in sediment accumulation rates in Adventfjorden, Svalbard. Oceanologia 46, 217–231.